

LEVEL

TR 4999-0003
MARCH 1980

6
Sc

EVALUATING THE SEADYN MODEL: MOORING DYNAMICS EXPERIMENT FIVE

By

DAVID B. DILLON

DTIC
ELECTE
MAR 21 1980
C

Prepared for

Civil Engineering Laboratory
Naval Construction Battalion Center
Port Hueneme, California 93043

This document has been approved
for public release and sale; its
distribution is unlimited.

Under Contract
N00014-78-C-0273

DDG FILE COPY

EB&G WASHINGTON ANALYTICAL SERVICES CENTER, INC.

2150 FIELDS ROAD / ROCKVILLE, MARYLAND 20850

PHONE (301) 840-3000

80 3 20 051

TR 4999-0003

MARCH 1980

EVALUATING THE SEADYN MODEL: MOORING DYNAMICS EXPERIMENT FIVE

By

DAVID B. DILLON

Prepared for



Civil Engineering Laboratory
Naval Construction Battalion Center
Port Hueneme, California 93043

Under Contract
N00014-78-C-0273

SECURITY CLASSIFICATION OF THIS PAGE (When Data Entered)

DD FORM 1473
1 JAN 73

UNCLASSIFIED

SECURITY CLASSIFICATION OF THIS PAGE (When Data Entered)

UNCLASSIFIED

SECURITY CLASSIFICATION OF THIS PAGE (When Data Entered)

The MDE provided exceptionally detailed tension data at four points along the mooring. SEADYN reproduces the general features of these measurements with remarkable accuracy.

The SEADYN tension traces include spurious oscillations that mask details of the tension history. These oscillations are believed to result from the omission of material damping in the SEADYN algorithm. Inclusion of hysteresis in the material stress-strain function is expected to remove the oscillations.

Modeling the MDE mooring occurs in two steps. SEADYN is a general cable dynamics computer model, using the finite-element method. The SEADYN user is also modeler as he reduces the physical mooring to equivalent elements and spherical or cylindrical nodes. This requires considerable technical skills and intuition when, for example, the physical object at the node is a pile of sandbags on a pallet.

Accession For	
NTIS CNA&I	<input checked="checked" type="checkbox"/>
DDC TAB	<input type="checkbox"/>
Unannounced	<input type="checkbox"/>
Justification	<input type="checkbox"/>
By	
Dist. Method	
Approval	
Post	Special
PR	

UNCLASSIFIED

SECURITY CLASSIFICATION OF THIS PAGE (When Data Entered)

TABLE OF CONTENTS

	Page
LIST OF FIGURES	i
LIST OF TABLES	ii
ABSTRACT	iii
 Section	
1 INTRODUCTION AND SUMMARY	1-1
2 MOORING DYNAMICS EXPERIMENT FIVE	2-1
3 MODEL DESCRIPTION	3-1
3.1 The SEADYN Model	3-1
3.2 The User as Modeler	3-1
3.3 The MDE Input Model	3-3
4 MODEL RESULTS AND COMPARISONS	4-1
4.1 Snapshot Geometry Comparisons	4-1
4.2 Trajectory Comparisons	4-1
4.3 Tension Comparisons	4-4
4.4 Computer Aspects	4-10
5 CONCLUSIONS	5-1
REFERENCES	R-1
 APPENDIX	
A Modeling MDE Experiment Five for SEADYN	A-1

LIST OF FIGURES

Figure		
2-1	Schematic Drawing of the Civil Engineering Laboratory Mooring	2-2

LIST OF FIGURES (cont'd)

Figure		Page
2-2	Ship Track and Experiment Location for CEL Mooring	2-3
2-3	Deployment Configuration "Snapshots" of CEL Mooring . . .	2-4
2-4	MDE: Tension at FVR 1 During Deployment	2-7
2-5	MDE: Tension at FVR 2 During Deployment	2-8
2-6	MDE: Tension at FVR 3 During Deployment	2-9
2-7	MDE: Tension at FVR 4 During Deployment	2-10
3-1	SEADYN Input Data Deck	3-4 & 3-5
3-2	The SEADYN Model of MDE Experiment Five	3-6
4-1	Cable Shape at Selected Times	4-2
4-2	Trajectories of Major nodes	4-3
4-3	Trajectories of Major Nodes (Composite)	4-5
4-4	Calculated Tension in Element Twenty-One (FVR 1)	4-6
4-5	Calculated Tension in Element Thirteen (FVR 2)	4-7
4-6	Calculated Tension in Element Eight (FVR 3)	4-8
4-7	Calculated Tension in Element Three (FVR 4)	4-9
4-8	Tension Comparison for FVR 1	4-12
4-9	Tension Comparison for FVR 2	4-13
4-10	Tension Comparison for FVR 3	4-14
4-11	Tension Comparison for FVR 4	4-15

LIST OF TABLES

Table		
2-1	Static Tension Distribution	2-6
A-1	Nodal Parameters	A-3

ABSTRACT

The computer model of ocean cable structures, SEADYN was used to calculate the anchor-last deployment of the sixth mooring (experiment five) of the Mooring Dynamics Experiment (MDE) conducted in Hawaiian waters in 1976. Comparisons are drawn with measurements of configuration and tension made during the deployment. The SEADYN configuration correlated well with the experimental data when an anchor drag coefficient of 0.78 was used. This value was precalculated to produce the terminal velocity experienced in the MDE.

The MDE provided exceptionally detailed tension data at four points along the mooring. SEADYN reproduces the general features of these measurements with remarkable accuracy.

The SEADYN tension traces include spurious oscillations that mask details of the tension history. These oscillations are believed to result from the omission of material damping in the SEADYN algorithm. Inclusion of hysteresis in the material stress-strain function is expected to remove the oscillations.

Modeling the MDE mooring occurs in two steps. SEADYN is a general cable dynamics computer model, using the finite-element method. The SEADYN user is also modeler as he reduces the physical mooring to equivalent elements and spherical or cylindrical nodes. This requires considerable technical skills and intuition when, for example, the physical object at the node is a pile of sandbags on a pallet.

SECTION I

INTRODUCTION AND SUMMARY

The design, construction and installation of large oceanic cable structures form a complex, expensive undertaking. In order to reduce the engineering uncertainties in the design of these structures, the Civil Engineering Laboratory, under the sponsorship of the Naval Facilities Engineering Command, is engaged in a major program to develop techniques for the static and dynamic analysis of oceanic cable structures.¹

This program is divided, on the one hand, into a series of small and large scale experiments to measure the response of cable structures to their dynamic environment, and on the other hand, into the development and evaluation of analytical tools, primarily computer programs, which attempt to predict those responses.

The first experiment in the series used an elastic strand about six feet long.² The second experiment used a similar silicone strand about sixty feet long, suspended in a laboratory tank.³ The third experiment used a 2,500 foot single point mooring set as part of the Mooring Dynamics Experiment (MDE) conducted at the Pacific Missile Range Facility, Barking Sands, Kauai, Hawaii in October, 1976.⁴

This report describes the modeling of the anchor-last deployment of MDE mooring number six using the general finite element program SEADYN as installed on a Control Data Corporation model 7600 computer.⁵ The report has been prepared for the Civil Engineering Laboratory (CEL) by EG&G Washington Analytical Services Center, Inc. under contract N00014-78-C-0273, using the SEADYN code provided by CEL.

¹ Superscripts identify references by number

SECTION 2

MOORING DYNAMICS EXPERIMENT FIVE

Figure 2-1 is a sketch of mooring number six in the Mooring Dynamics Experiment⁵ series. It is a submerged single point mooring instrumented to record tensions at four locations along the cable, the positions of four nearby points, as well as the water temperature and hydrostatic pressure at two other locations. The instruments were set to record before, during, and after the deployment sequence.

This report is concerned with the dynamics of the mooring during its deployment using the anchor-last technique. In this method, the uppermost float is released first from the deploying vessel. The buoy floats on the sea surface and is towed by the mooring cable from the deploying ship. The mooring is paid out and instruments are attached as the ship steams slowly on a straight course until only the anchor remains on deck. When the stern passes over the desired mooring point, the anchor is cast overboard, and plummets essentially straight to the bottom, dragging the top float down with it. Figure 2-2 shows the deployment track and mooring location for the CEL mooring.

Figure 2-3 shows the measured shape of the cable arc for five times during the deployment, at two-minute intervals. Just before the anchor was released, the mooring streamed in a flat catenary, suspended at its top end by the buoy floating on the sea surface and at its anchor end by the deployment ship, USNS De Steiguer (T-AGOR-12). Time 5310 is shortly before the anchor was released. Time 5480 shows the mooring early in the descent. Times 5550 and 5670 show the anchor falling nearly vertically and dragging the mooring buoy to the mooring point. Time 6120 shows the anchor on the bottom, with the mooring essentially vertical above it. Note that as the mooring cable came towards the vertical after 5670 seconds, its horizontal drag became great enough to deflect the anchor's path about 250 feet back in the direction of the upper sphere.

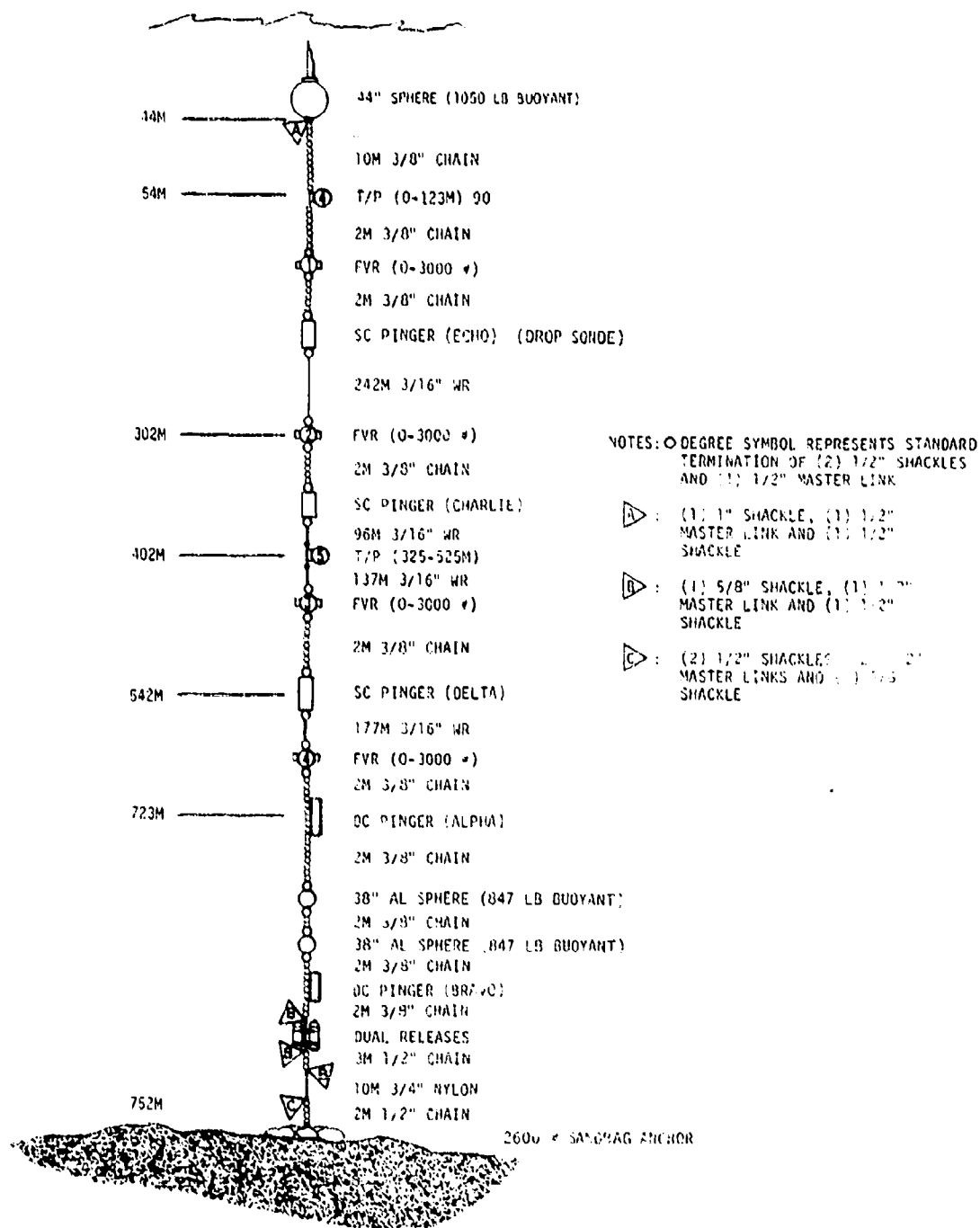


Figure 2-1. Schematic Drawing of the Civil Engineering Laboratory Mooring

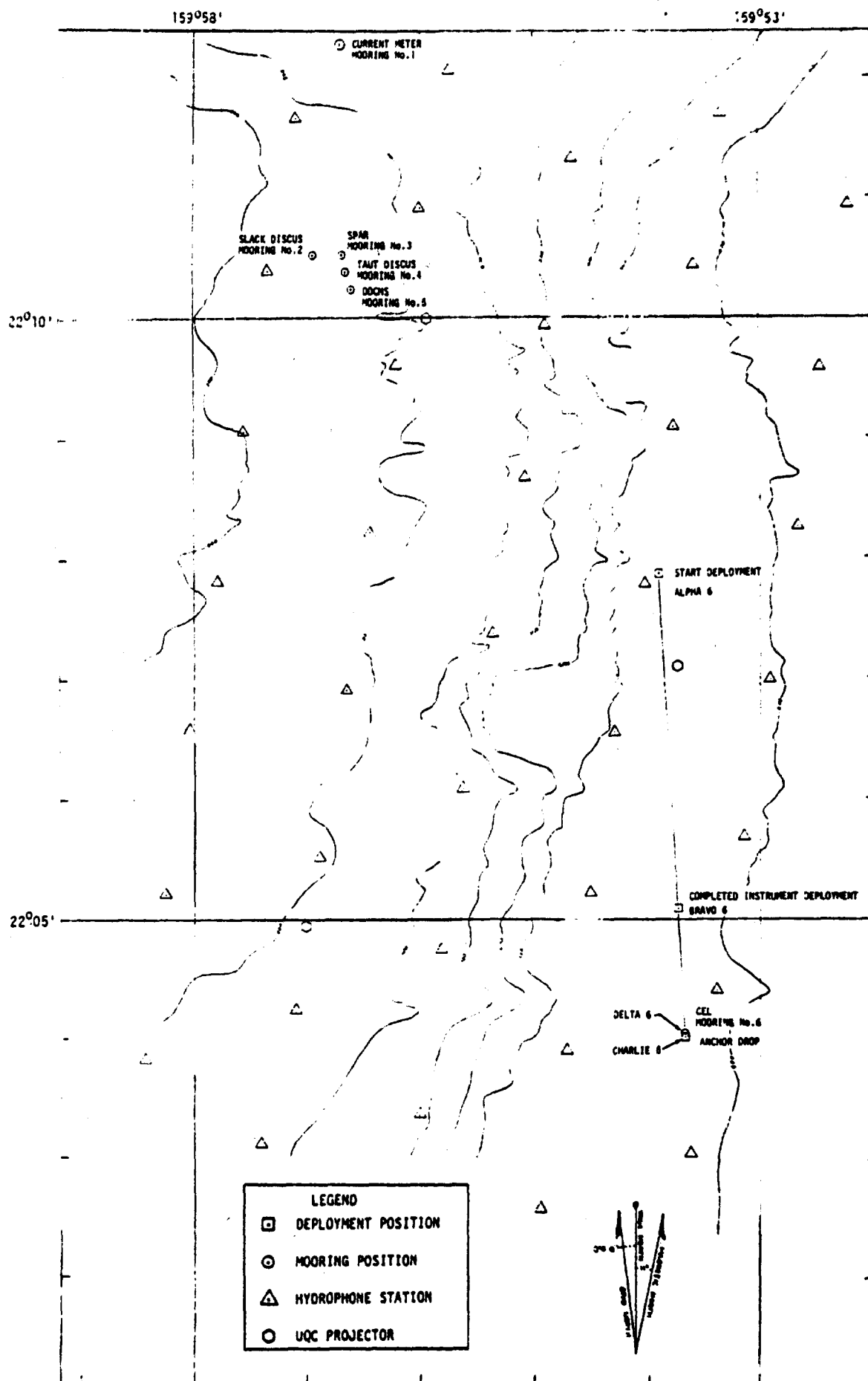


Figure 2-2. Ship Track and Experiment Location
for CEL Mooring

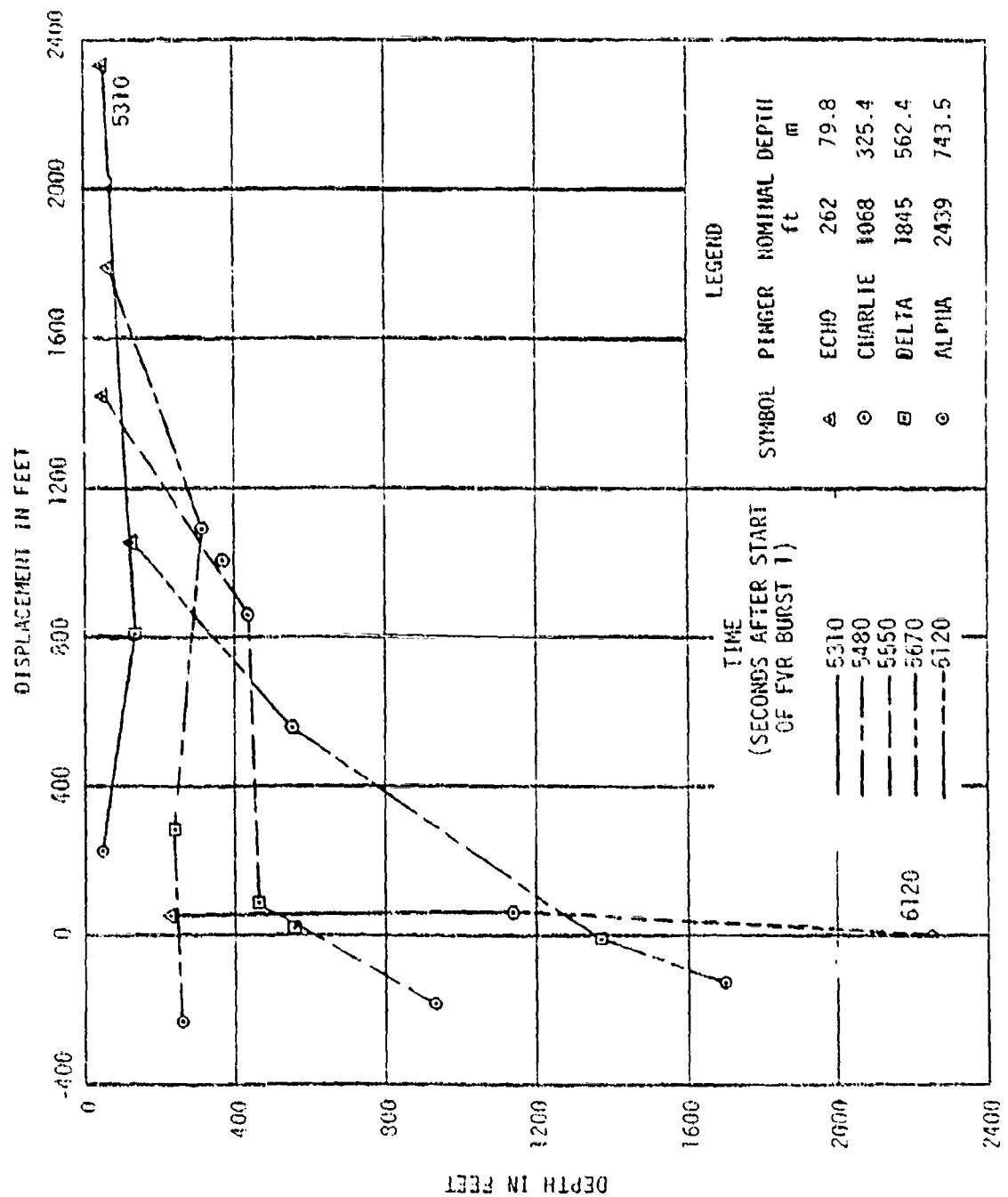


Figure 2-3. Deployment Configuration "Snapshots" of CEL Mooring

After the mooring deployment is complete, the cable hangs in a nearly vertical line, so that the tension can be calculated by summing the immersed weights of the components. This affords a check on the accuracy of the tensiometers installed on the mooring. Table 2-1 shows the tension to be expected at each tensiometer (FVR = Force Vector Recorder) based on summing of weight/buoyancy and the values read from the tension plots. The FVR readings are always within five percent of the weighed values - which themselves are probably not better than five percent. Figures 2-4 through 2-7 show the data from FVR's one through four. The FVR traces show such a detailed history of the deployment that it is worthwhile to quote the qualitative analysis given in Reference 4*.

"The tension records produced by the four FVR's during the mooring deployment represent a remarkable achievement in the history of ocean mechanical experimentation. This degree of clarity and agreement among the four instruments has rarely been achieved in at-sea trials. The resulting plots are so clear that qualitative interpretation is straightforward.

"During the two minute portion of the trace before the anchor was released, all the traces show a constant tension with wave-induced variations superimposed. The constant tension is due to the steady towing speed of the De Steiguer plus the weight and buoyancy of the components. The average tension at the anchor end (FVR 4) is highest, since all the towing drag and a good share of the weight are supported there. The average tension at FVR 3 is somewhat less, since it supports less weight and less drag. The average tension at FVR 2 is less still. FVR 2 is apparently near the deepest part of the "catenary" of the mooring under tow. The average tension at FVR 1 is essentially the same as at FVR 2, because while it supports less drag, it supports more weight.

The large tension variation during this period is dominated by the motions of the De Steiguer in the seaway. This conclusion is supported by the reduction in tension amplitude from FVR 4 to FVR 1, away from the towing ship. It is further supported by the reduction in amplitude after the anchor is released and the ship cannot force the mooring.

* Section V, paragraph E, pp 9-11

TABLE 2-1. STATIC TENSION DISTRIBUTION

FVR	NOMINAL DEPTH (Ft)	STATIC* TENSION (Lb)	FVR READING (Lb)	SEADYN			ELEMENT
				MINIMUM (Lb)	MAXIMUM (Lb)	MEAN (Lb)	
1	92	969	985	985	985	985	21
2	935	877	840	710	930	820	13
3	1680	767	730	640	810	725	8
4	2280	685	700	550	730	640	3

* Estimated from immersed weights of components

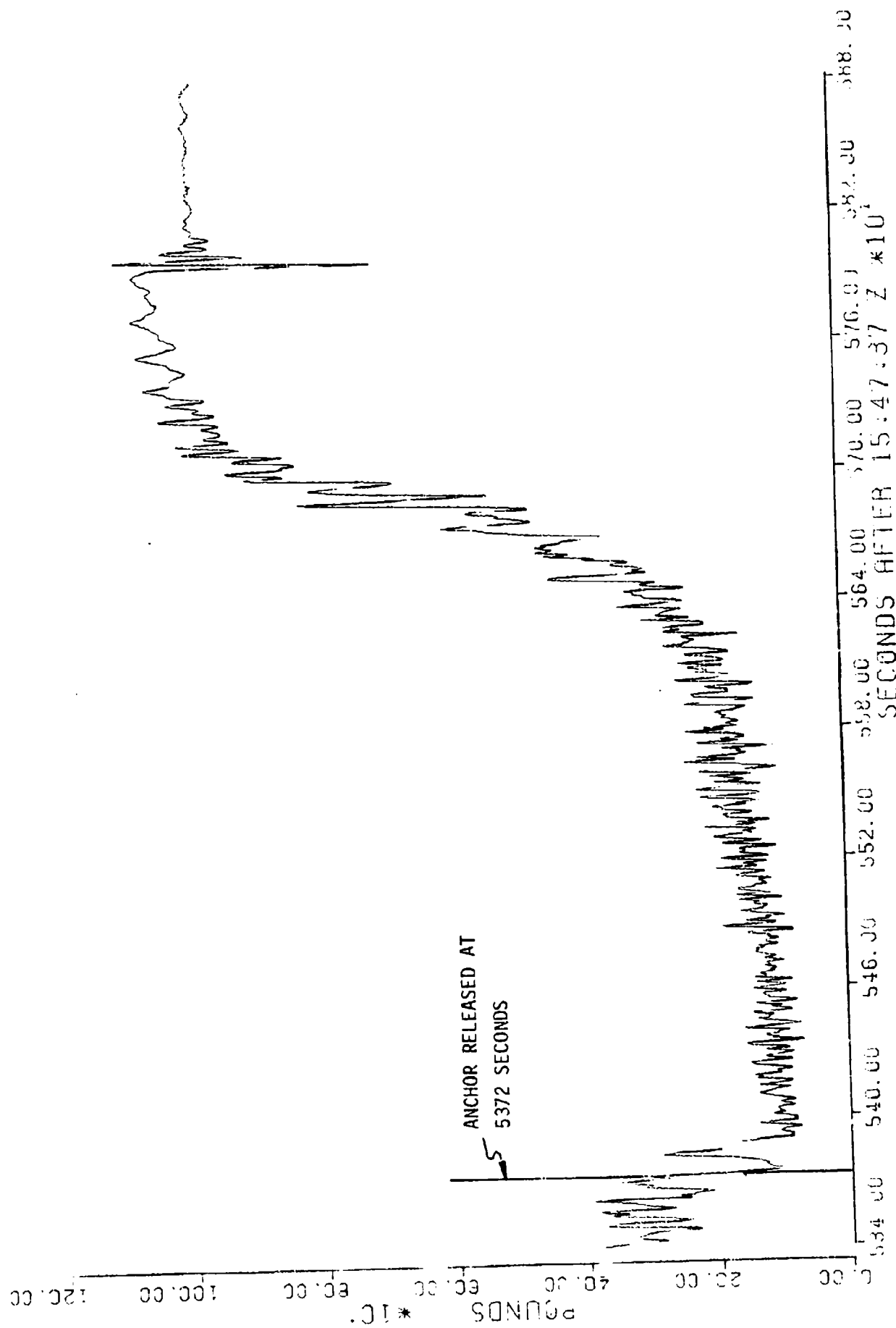


Figure 2-4. MDE: Tension at FVR 1 During Deployment

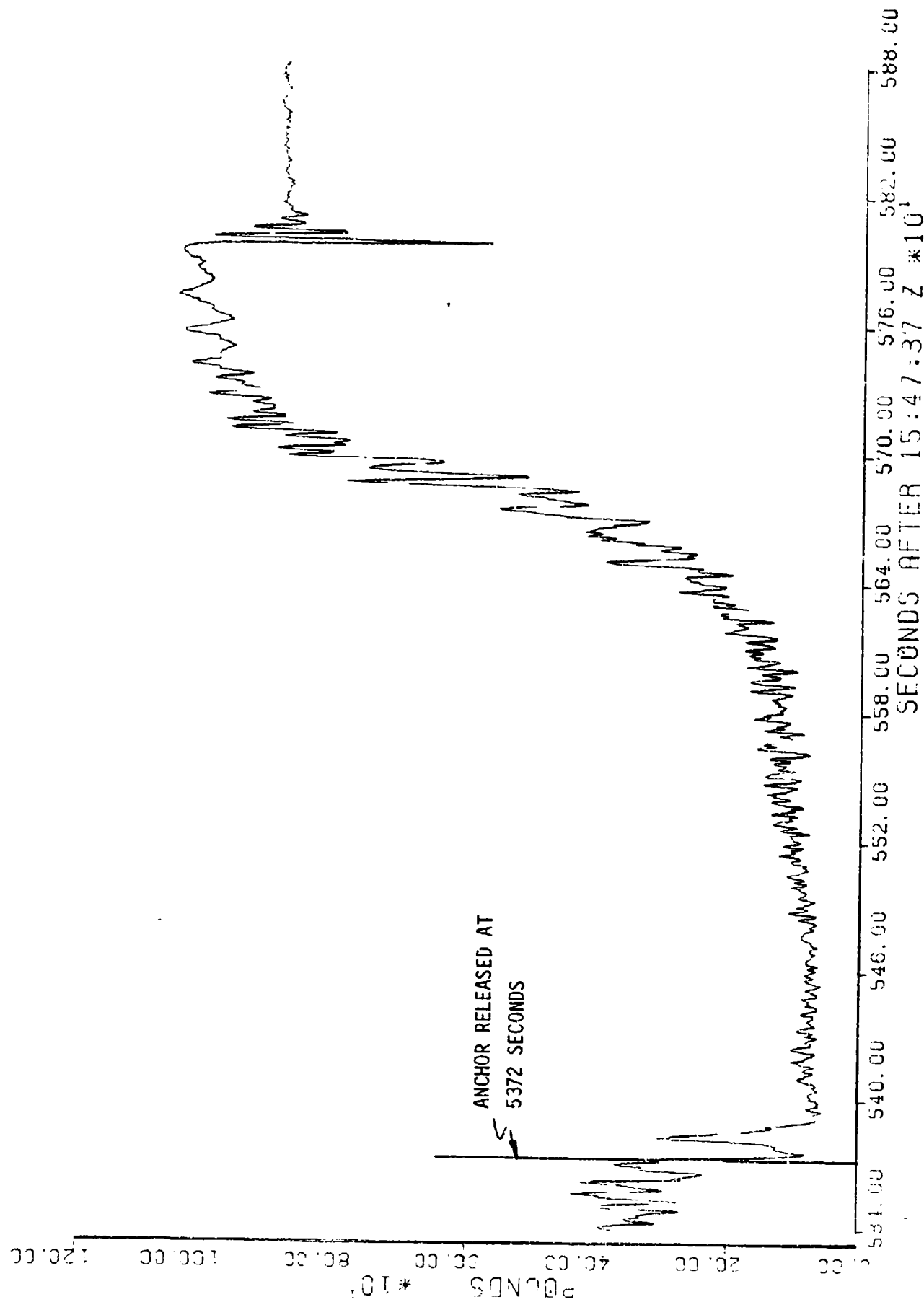


Figure 2-5. MDE: Tension at FVR 2 During Deployment

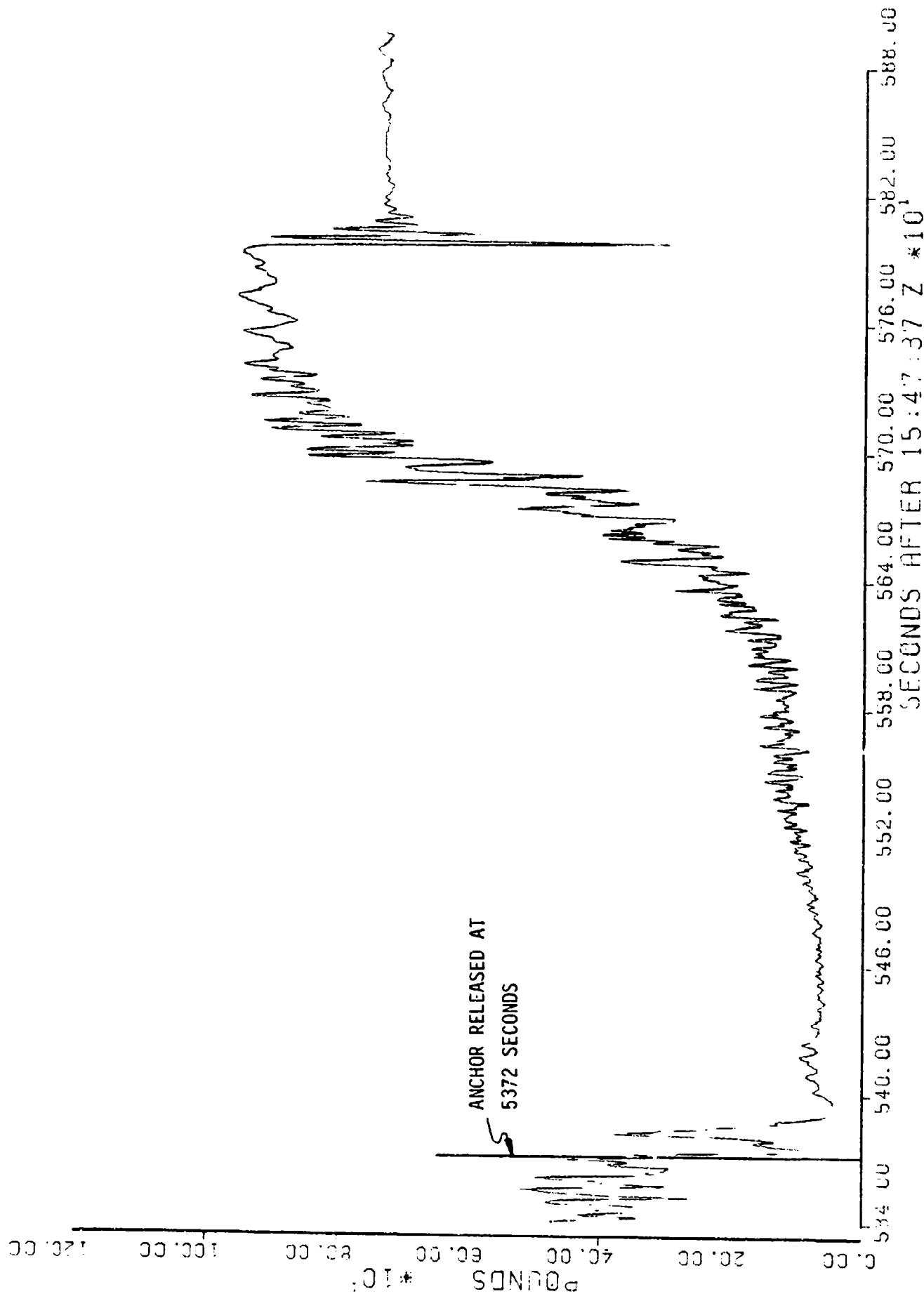


Figure 2-5. MDE: Tension at FVR 3 During Deployment

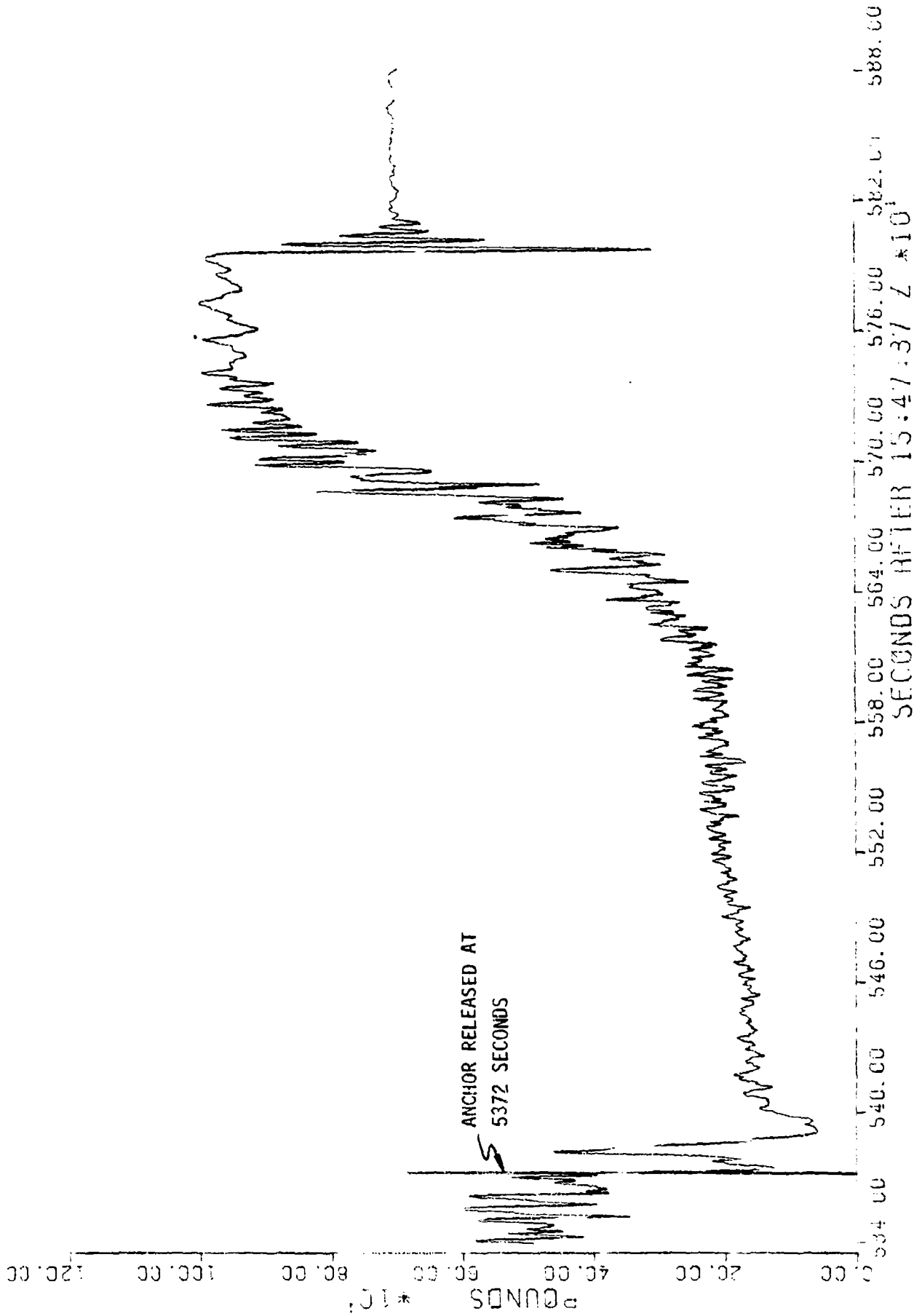


Figure 2-7. MDE: Tension at FVR 4 During Deployment

"The tension falls abruptly as the anchor is released, the drop-off being most abrupt at FVR 4 and less so at FVR 1, farthest from the anchor. One might speculate whether the "spikes" in the drop-off trace represent reflections of the initial tension wave produced at the moment of release.

"In any case about 30 seconds after the anchor has been released, at say 5400 seconds into the FVR record, a new equilibrium is established. FVR 1 shows (Figure 2-4) the tension required to tow the main buoy, afloat on the surface. The main float bobs on the waves, producing a spectrum like the pre-drop trace, but lacking the large low frequency spikes of the De Steiguer. These wave-induced pulses are much attenuated at FVR's 2, 3, and 4. FVR 2 is still near the bottom of the catenary, but because the anchor tows the float more slowly the drag is reduced between FVR 1 and FVR 2, but the weight does not change. The result is that the tension at FVR 2 (Figure 2-5) is less than at FVR 1 (Figure 2-4). The tension at FVR 3 (Figure 2-6) is essentially the same, but at FVR 4 (Figure 2-7) the entire towing drag is felt.

"This equilibrium lasts for about three minutes, showing the "water pulley" effect whereby the cable tends to resist transverse motion and follow tangential motion, as if the water were a great pulley sheave. By about 5460 seconds into the FVR record, the "sheave" has been "worn away", and the anchor is beginning to pull the main buoy down with an ever-increasing force. During the next minutes the buoy becomes nearly directly above the anchor and the tension rises sharply to the maximum buoyancy of the main float as the buoy comes awash. During this time the wave induced oscillations are much greater, because the vertical motion of the buoy on the waves couples directly into the nearly vertical cable. At about 5730 seconds the buoy comes awash, and immediately the effects of small surface waves disappear. Only the swell remains, and its amplitude decreases as the buoy descends. The mean tension is set by the buoyancy and drag of the main float as it is towed down at the system terminal velocity. By comparing the four figures, the distribution of weight along the mooring becomes apparent during this minute of near-equilibrium.

"The impact of the anchor and its decay in time are clearly shown on each FVR trace; its decay with distance along the cable is also apparent, since the oscillations at FVR 1 are about half those at FVR 4.

"Following impact, the tension produced by the drag of falling at terminal speed is removed, and only the nudgings of the swell on the main float remain.

"These remarkable traces represent a convincing test for the validity of a mooring dynamics prediction model."

The log of the experiment shows the anchor released at 17:17 GMT. This is 5430 seconds after the start of the first recording "burst" of the FVR's at 15:47:37 GMT. The traces on Figures 2-4 through 2-7 thus commence with the nominal release of the anchor. However, the traces themselves suggest that the anchor was released somewhat later, but the exact moment is obscured by the sea state. Reference four includes five other pertinent data records from the experiment - depth and temperature histories for two T/P recorders, as well as the depth of pinger alpha, nearest the anchor. The low frequency T/P trace has a "kink" at 17:17:30 \pm 30 seconds GMT. The high frequency T/P traces indicate that the anchor was released at 17:17:30 \pm 10 seconds GMT. Using 17:17:30 GMT as a guidepost, the depth history of pinger alpha yields a likely anchor release time of 17:17:32 \pm 2 seconds GMT, that is 5372 \pm 2 seconds after 15:47:37 GMT.

SECTION 3

MODEL DESCRIPTION

3.1 The SEADYN Model

Reference five includes a description of the theoretical structure of the SEADYN computer program. SEADYN is a finite-element model of a cable network using large-displacement, non-linear elastic theory. It is easy to think of the SEADYN code as the model, so that if the results of the MDE comparison, as well as the others in the series of validations, are favorable, then SEADYN is a valid model for ocean cable systems. And that is true. But from a practical standpoint there is another, more important, model to be considered.

3.2 The User as Modeler

That model is defined by the set of data that the user supplies as input to SEADYN. It is more important, because the input model is not created by a highly trained expert who has had the opportunity to check and recheck his analysis over an extended period of time. The input model is created by the user. It is specific to the problem, but it is far from being a unique representation of the cable system to SEADYN. A cable system can be presented to SEADYN in a multitude of ways. Many will give essentially equivalent results, but many others may produce erroneous results, or even prevent SEADYN from reaching a solution at all. The validity of the input model depends on the knowledge, skill, patience, and care of the user.

The input model is more important than the analytical model because it cannot be validated in advance, once and for all, by any series of test cases. Every new problem represents a new challenge. Over a period of time, individual users will develop skill and experience, and may communicate this effectively with other users.

SEADYN treats a cable system as a network of cables whose ends are linked together or attached to external objects. This may be something very complex, like a spider web, or quite simple, as the MDE mooring. With the MDE/CEL mooring the cable elements are all connected in series, end to end, from the anchor to the main buoy. The junctions of cable ends are called nodes. Rigid objects may be attached at nodes. The first way the user influences the input model is by selecting the number and distribution of nodes.

SEADYN accepts rigid bodies attached at nodes. Ships and surface buoys may have nodes attached at several different locations, so that these bodies are handled by the SEADYN geometry. However, SEADYN has a restricted repertoire of physical shapes for which it can calculate hydrodynamic drag and added mass forces. The user must translate the drag and added mass of irregular shapes into equivalent coefficients or add subroutine codes to calculate appropriate values. This is a considerable technical problem, and may require in-water tests of physical models of irregular shapes to determine appropriate values. Selection of these equivalencies can strongly affect the rate of dynamic processes - speeds and frequencies - calculated by SEADYN.

The third interaction of the user with the input model is due to the direct relation between element length and time step. The conservative user will seek to use a large number of small elements. But this forces him concurrently to specify a small time step size - indeed, if he does not, SEADYN will do it for him. But the amount of computer resources needed grows rapidly as the number of elements goes up and the time step gets smaller.

For example, simulating the MDE deployment, an event lasting about nine minutes, required more than 25 minutes on the CDC 7600 processor, which approximates the current state-of-the-art for commercially available computation. The MDE input model used 21 elements connecting 22 nodes serially - the most efficient linkage. Had the number of elements been doubled, then the time step would be halved. The computer would do twice as many computations per time step for twice as many steps: quadruple the computer time. The user can specify a prohibitively expensive input model. On the other hand, if too few elements are used, the user may lose important details of the system dynamics.

Fourth, SEADYN is a very general computer program, with many options. Becoming usefully familiar with these options is not a trivial task in itself. In addition, however, a given problem often can be solved using more than one combination of options. Some of these options are very far reaching, extending even to the mathematical algorithm that SEADYN will employ.

3.3 The MDE Input Model

Figure 3-1 is the input model used to calculate the deployment of the MDE/CEL mooring. Each line of numbers and text on Figure 3-1 is an image of an 80-column punched computer card. The three-digit number at the left of each line is not a part of the card image, nor is the text-label that ends each line on the right. The last line (690) is presented as a convenience in locating entries on the card format.

A detailed discussion of each entry on Figure 3-1 is beyond the scope of this report. Reference 5 contains a description of each input parameter. The node cards (040 through 250) give initial estimates of the locations of the 22 nodes of the MDE/CEL model at the instant the anchor was dropped. The lengths of the 21 elements are calculated from these nodal positions. Cards 260 through 290 identify the kind of cable used in each element, while cards 300 through 390 give the characteristics of each kind of cable. Cards 400 through 550 specify the rigid body properties for the nodes in terms of equivalent spheres and cylinders. Appendix A gives the derivation of these values. Cards 560 through 630 instruct SEADYN to find the shape of the mooring as it is towed behind the ship just as the anchor is dropped. Finally, cards 640 through 670 control the analysis of the deployment. Card 680 stops SEADYN. Figure 3-2 is a sketch, not to scale, of the equivalent mooring input to SEADYN.

010	0.8.	OILLON	ANALYSIS OF MDE EXPT 5 DEPLOYMENT USING SEADYN										PROBLEM TITLE		
020	22	0	0	0	21	3	8	0	-1	0	1	1	0	0	MASTER CONTRL
030	2	1	32.1725	1.2871E-5	64.3394	0.	0.	0.	0.	0.	0.	0.	0.	0.	ENVIRONMENT
040	1	0	-0.00			0.	0.	0.	0.	0.	0.	0.	0.	0.	ANCHOR NODE
050	2	0	-32.82			0.	0.	0.	0.	0.	0.	0.	0.	0.	RELEASE NODE
060	3	0	-124.33			0.	0.	0.	0.	0.	0.	0.	0.	0.	FVR-4 NODE
070	4	0	-222.83			0.	0.	0.	0.	0.	0.	0.	0.	0.	WIRE NODE
080	5	0	-341.34			0.	0.	0.	0.	0.	0.	0.	0.	0.	WIRE NODE
090	6	0	-459.84			0.	0.	0.	0.	0.	0.	0.	0.	0.	WIRE NODE
100	7	0	-578.35			0.	0.	0.	0.	0.	0.	0.	0.	0.	WIRE NODE
110	8	0	-636.85			0.	0.	0.	0.	0.	0.	0.	0.	0.	FVR-3 NODE
120	9	0	-847.22			0.	0.	0.	0.	0.	0.	0.	0.	0.	WIRE NODE
130	10	0	-997.59			0.	0.	0.	0.	0.	0.	0.	0.	0.	WIRE NODE
140	11	0	-1147.96			0.	0.	0.	0.	0.	0.	0.	0.	0.	T/P-5 NODE
150	12	0	-1311.18			0.	0.	0.	0.	0.	0.	0.	0.	0.	WIRE NODE
160	13	0	-1474.40			0.	0.	0.	0.	0.	0.	0.	0.	0.	FVR-2 NODE
170	14	0	-1575.12			0.	0.	0.	0.	0.	0.	0.	0.	0.	WIRE NODE
180	15	0	-1675.84			0.	0.	0.	0.	0.	0.	0.	0.	0.	WIRE NODE
190	16	0	-1776.56			0.	0.	0.	0.	0.	0.	0.	0.	0.	WIRE NODE
200	17	0	-1877.29			0.	0.	0.	0.	0.	0.	0.	0.	0.	WIRE NODE
210	18	0	-1978.01			0.	0.	0.	0.	0.	0.	0.	0.	0.	WIRE NODE
220	19	0	-2078.73			0.	0.	0.	0.	0.	0.	0.	0.	0.	WIRE NODE
230	20	0	-2179.45			0.	0.	0.	0.	0.	0.	0.	0.	0.	WIRE NODE
240	21	0	-2280.17			0.	0.	0.	0.	0.	0.	0.	0.	0.	FVR-1 NODE
250	22	0	-2323.64			0.	0.	0.	0.	0.	0.	0.	0.	0.	SPHERE NODE
260	1	1	2	1	0	0	300.	1	0	0	0	0.	0.	0.	NYLON ELEMENT
270	2	2	3	2	0	0	300.	0	0	0	0	0.	0.	0.	CHAIN ELEMENT
280	3	3	4	3	0	0	300.	0	0	0	0	0.	0.	0.	WIRE ELEMENT
290	21	21	22	2	0	1	300.	0	0	0	0	0.	0.	0.	CHAIN ELEMENT
300	1	0	.0625	.017			1.	5	0	0	0	0.	0.	0.	NYLON MATERIAL
310		4.	.001												STRAIN 1-1
320		895.	.153												STRAIN 1-2
330		1640.	.230												STRAIN 1-3
340		4250.	.305												STRAIN 1-4
350		6860.	.340												STRAIN 1-5

Figure 3-1. SEADYN Input Data Deck

	CHAIN MATERIAL	SIRAIN 2-1	WIRE MATERIAL	SIRAIN 3-1	ANCHOR SPECS	EXTRA SPECS	RELEASE SPECS	EXTRA SPECS	FVR-4 SPECS	EXTRA SPECS	FVR-3 SPECS	EXTRA SPECS	T/P-5 SPECS	EXTRA SPECS	FVR-2 SPECS	EXTRA SPECS	FVR-1 SPECS	EXTRA SPECS	SPHERE SPECS	EXTRA SPECS	SUBANALYSIS	SOLUTION	CURRENT	FIX ANCHOR-X	FIX ANCHOR-Y	FIX RELEASE-Y	FIX FVR 4-Y	FIX SPHERE-Y	SUBANALYSIS	SOLUTION	TIME DATA	INITIAL VELOCITY	
360	2	1	.03125	2.743	2.	0	0	0	0	0	0	0	0	0	0	0	0	0	0	0	0	0	0	0	0	0	0	0	0	0	0	0	
370	1	26E+6	1.																														
380	3	0	.0325	.05374	1.	0	0	0	0	0	0	0	0	0	0	0	0	0	0	0	0	0	0	0	0	0	0	0	0	0	0	0	
390	3	44E+5	1.																														
400	1	2	-2600.	4.0	0.	0	0	0	0	0	0	0	0	0	0	0	0	0	0	0	0	0	0	0	0	0	0	0	0	0	0	0	
410	0		7.354	0.	1.0001	1	0	0	0	0	0	0	0	0	0	0	0	0	0	0	0	0	0	0	0	0	0	0	0	0	0	0	
420	2	2	511.1	4.562	0.	0	0	0	0	0	0	0	0	0	0	0	0	0	0	0	0	0	0	0	0	0	0	0	0	0	0	0	
430	0		9.568	0.	1.0001	0	0	0	0	0	0	0	0	0	0	0	0	0	0	0	0	0	0	0	0	0	0	0	0	0	0	0	
440	3	2	790.3	3.917	0.	0	0	0	0	0	0	0	0	0	0	0	0	0	0	0	0	0	0	0	0	0	0	0	0	0	0	0	
450	0		7.051	0.	1.0001	0	0	0	0	0	0	0	0	0	0	0	0	0	0	0	0	0	0	0	0	0	0	0	0	0	0	0	
460	8	2	-49.95	2.149	0.	0	0	0	0	0	0	0	0	0	0	0	0	0	0	0	0	0	0	0	0	0	0	0	0	0	0	0	
470	0		2.123	0.	1.0001	0	0	0	0	0	0	0	0	0	0	0	0	0	0	0	0	0	0	0	0	0	0	0	0	0	0	0	
480	11	0	-19.92	0.958	0.	0	0	0	0	0	0	0	0	0	0	0	0	0	0	0	0	0	0	0	0	0	0	0	0	0	0	0	
490	0		0.270	0.	1.0001	0	0	0	0	0	0	0	0	0	0	0	0	0	0	0	0	0	0	0	0	0	0	0	0	0	0	0	
500	13	2	-49.95	2.149	0.	0	0	0	0	0	0	0	0	0	0	0	0	0	0	0	0	0	0	0	0	0	0	0	0	0	0	0	
510	0		2.123	0.	1.0001	0	0	0	0	0	0	0	0	0	0	0	0	0	0	0	0	0	0	0	0	0	0	0	0	0	0	0	
520	21	2	-59.75	2.210	0.	0	0	0	0	0	0	0	0	0	0	0	0	0	0	0	0	0	0	0	0	0	0	0	0	0	0	0	
530	0		2.245	0.	1.0001	0	0	0	0	0	0	0	0	0	0	0	0	0	0	0	0	0	0	0	0	0	0	0	0	0	0	0	
540	22	0	1046.2	3.657	0.	0	0	0	0	0	0	0	0	0	0	0	0	0	0	0	0	0	0	0	0	0	0	0	0	0	0	0	
550	0		3.960	0.	1.0001	0	0	0	0	0	0	0	0	0	0	0	0	0	0	0	0	0	0	0	0	0	0	0	0	0	0	0	
560	LIVE	1	1	0	1	0	5	0	0	0	-1	200	21	0	0	0	0	0	0	0	0	0	0	0	0	0	0	0	0	0	0	0	
570		0.1	.0001	.0001	1.	0	.5	0	0	0	0	.5	0	0	0	0	0	0	0	0	0	0	0	0	0	0	0	0	0	0	0	0	
580	-5.483		0.	0.	0.																												
590	1	1	0.	1	0.	1	0	0	0	0	0	0	0	0	0	0	0	0	0	0	0	0	0	0	0	0	0	0	0	0	0	0	
600	1	2	0.	1	0.	1	0	0	0	0	0	0	0	0	0	0	0	0	0	0	0	0	0	0	0	0	0	0	0	0	0	0	
610	2	2	0.	1	0.	1	0	0	0	0	0	0	0	0	0	0	0	0	0	0	0	0	0	0	0	0	0	0	0	0	0	0	
620	3	2	0.	1	0.	1	0	0	0	0	0	0	0	0	0	0	0	0	0	0	0	0	0	0	0	0	0	0	0	0	0	0	
630	22	2	0.	1	0.	1	0	0	0	0	0	0	0	0	0	0	0	0	0	0	0	0	0	0	0	0	0	0	0	0	0	0	
640	0YM	1	1	0	0	0	0	0	0	0	0	0	0	0	0	0	0	0	0	0	0	0	0	0	0	0	0	0	0	0	0	0	
650		.01	-.0001	-.0001	0.	0	0	0	0	0	0	0	0	0	0	0	0	0	0	0	0	0	0	0	0	0	0	0	0	0	0	0	
660		.005	.5	10.	.5	.08333333	0.	0	0	0	0	0	0	0	0	0	0	0	0	0	0	0	0	0	0	0	0	0	0	0	0	0	
670		5.483	0.	0.	0.																												
680	END 0	1	1	2	3	3	4	4	5	5	5	6	7	7	7	7	7	7	7	7	7	7	7	7	7	7	7	7	7	7	7	7	
690	122455789012345578901																																

Figure 3-1. SEADYN Input Data Deck (Continued)

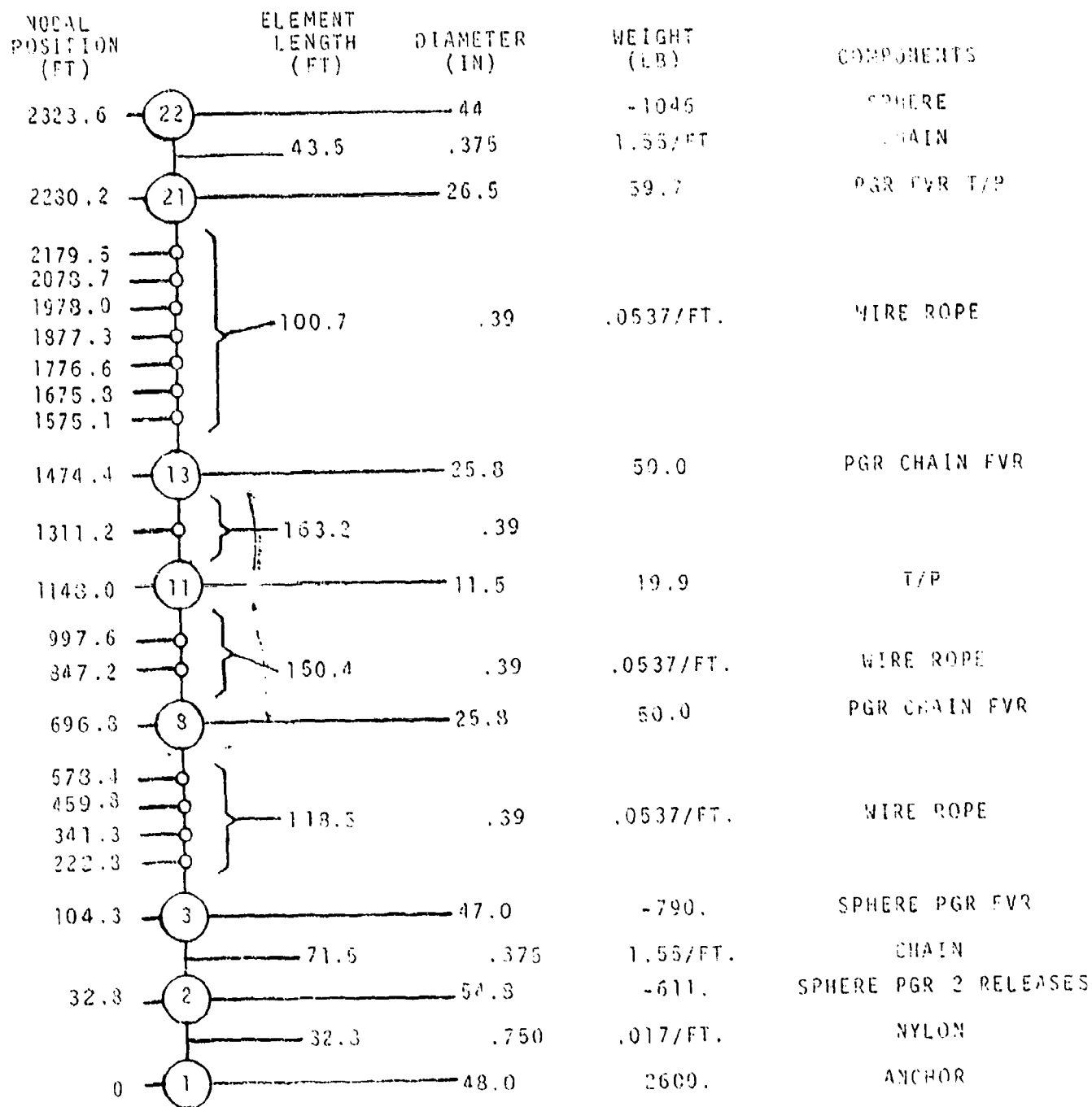


Figure 3-2. The SEADYN Model of MDE Experiment Five

SECTION 4

MODEL RESULTS AND COMPARISONS

4.1 Snapshot Geometry Comparisons

Figure 4-1 shows the shape of the MDE/CEL mooring calculated at selected times during the deployment. At time $t=0$, the anchor is on the towship at the upper right corner of the figure, and the main buoy is on the water surface at the upper left corner of the figure.

Even though the ship is towing the mooring from left to right at 3.25 knots, the anchor does not coast an appreciable distance after release. Indeed, it swings back first, under the recovery buoys attached to the acoustic release. Then it falls nearly vertically down the right margin of the figure, until the main buoy is pulled under about six minutes (360 seconds) after release. Then the anchor begins a sedate pendulum-swing to the left under the main buoy until it impacts on the bottom during the eighth minute after release.

4.2 Trajectory Comparisons

Figure 4-2 shows the paths taken by major nodes during the deployment. The trajectories should be viewed individually; viewed collectively, they can be confusing. Start with the anchor at node one. Upon release it swings under the recovery buoys, pulling them under one after the other, then plummets straight down the right margin of the plot until the main buoy pulls under, when the anchor begins to swing to the left. Finally, it impacts on the bottom at a depth of 2465 feet.

FVR at node three coasts a moment after release, then is jerked under by the anchor and plummets down with it.

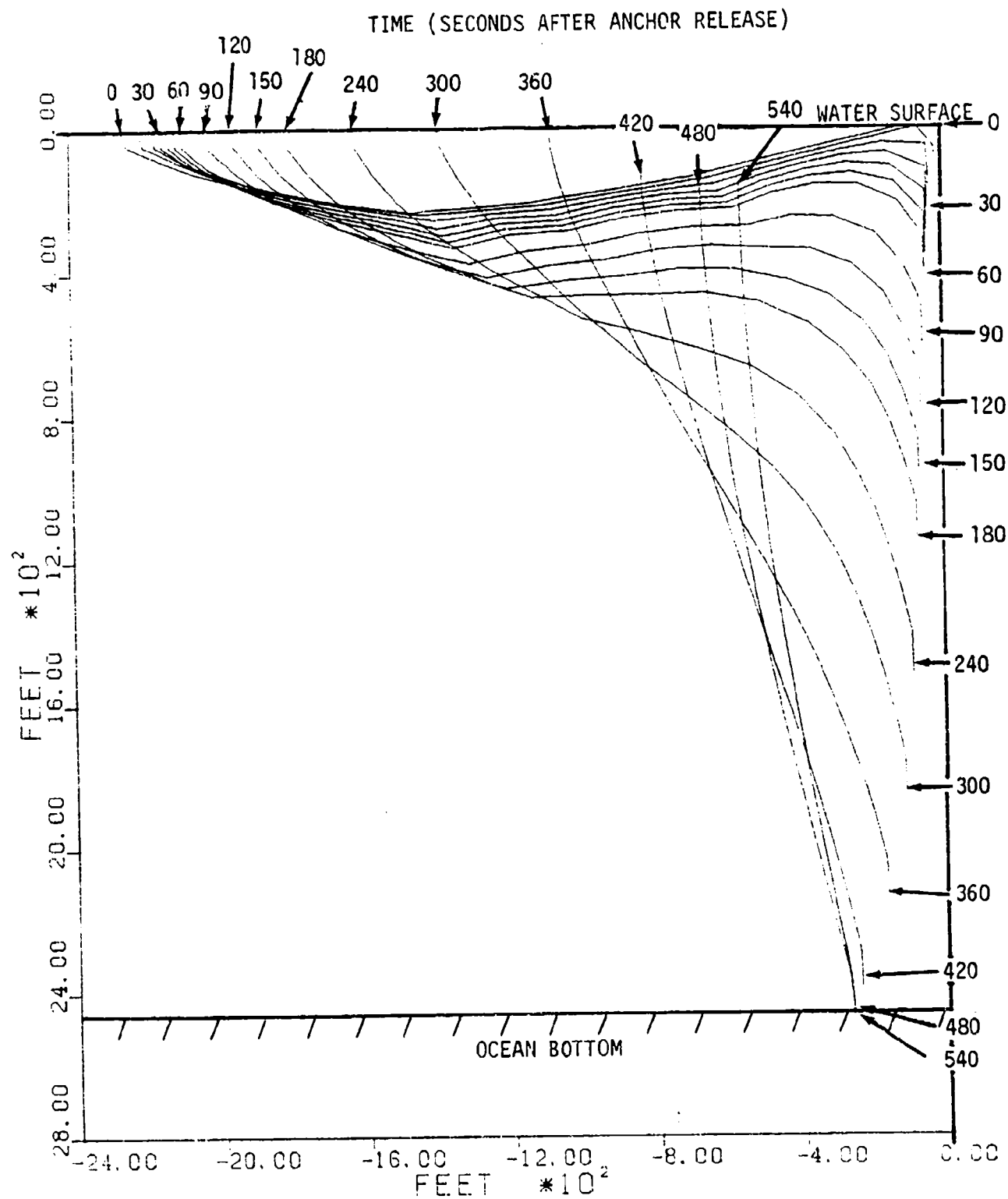


Figure 4-1. Cable Shape at Selected Times

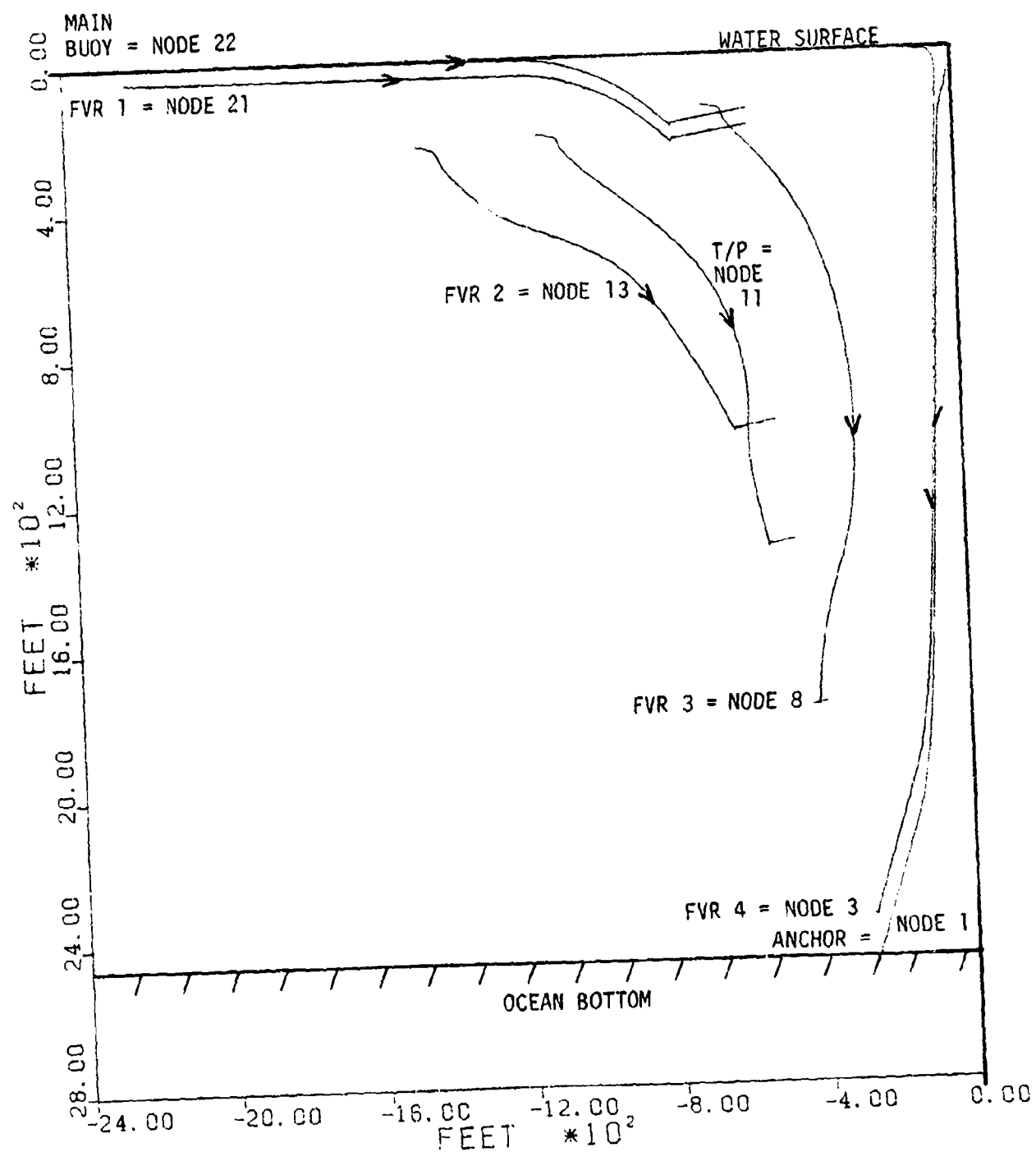


Figure 4-2. Trajectories of Major Nodes

FVR 3 at node eight, the temperature/pressure (T/P) sensor at node 11, and FVR 2 at node 13 all coast a little while, then are pulled down in sweeping arcs following the "water pulley" principle (The drag on a cable perpendicular to it is much greater than the drag tangent to the cable. When a cable is pulled sideways in the water, it tends to bend as if the water were a great pulley wheel. The cable tends to pull "around the corner" more than it "cuts across" the corner.) After the anchor hits bottom these three nodes abruptly stop falling and swing on arcs about the anchor as fixed point.

FVR 1 at node 21 and the main buoy at node 22 are towed along under or on the surface while the rest of the cable goes around the "water pulley." Then the anchor pulls the main buoy under, and shortly thereafter impacts. These nodes then pivot up and to the right about the anchor.

Figure 4-3 is a duplicate of Figure 4-2 with locations of the nodes measured during the MDE superimposed. It is easy to see the triangle symbols (pinger ECHO) closely paralleling the trajectory of node 21. The circle symbols (pinger ALPHA) follow node three behind the anchor. The square symbols (pinger DELTA) loosely follow node eight. The hexagons (pinger CHARLIE) clearly follow node 13.

4.3 Tension Comparisons

Figures 4-4 through 4-7 are the calculated equivalents to Figures 2-4 through 2-7. The resemblance is striking, except for the large oscillations of tension. The large tension pulse produced by the anchor impact is shown on Figures 2-4 through 2-7 to have decayed fully within 30 seconds; one may infer that other inputs decay in a like time. Therefore, the tension oscillations on those plots are primarily due to continuous excitation, namely the action of ocean waves.

The SEADYN model contained no simulation of wave action. One would therefore expect smooth tension traces with discrete perturbations lasting about 30 seconds coincident with anchor release, anchor impact, and perhaps the immersion of the main buoy. This is found to be the case for some elements some of the time: element eight from about 3.5 to 7 minutes after anchor release, for example, on Figure 4-6.

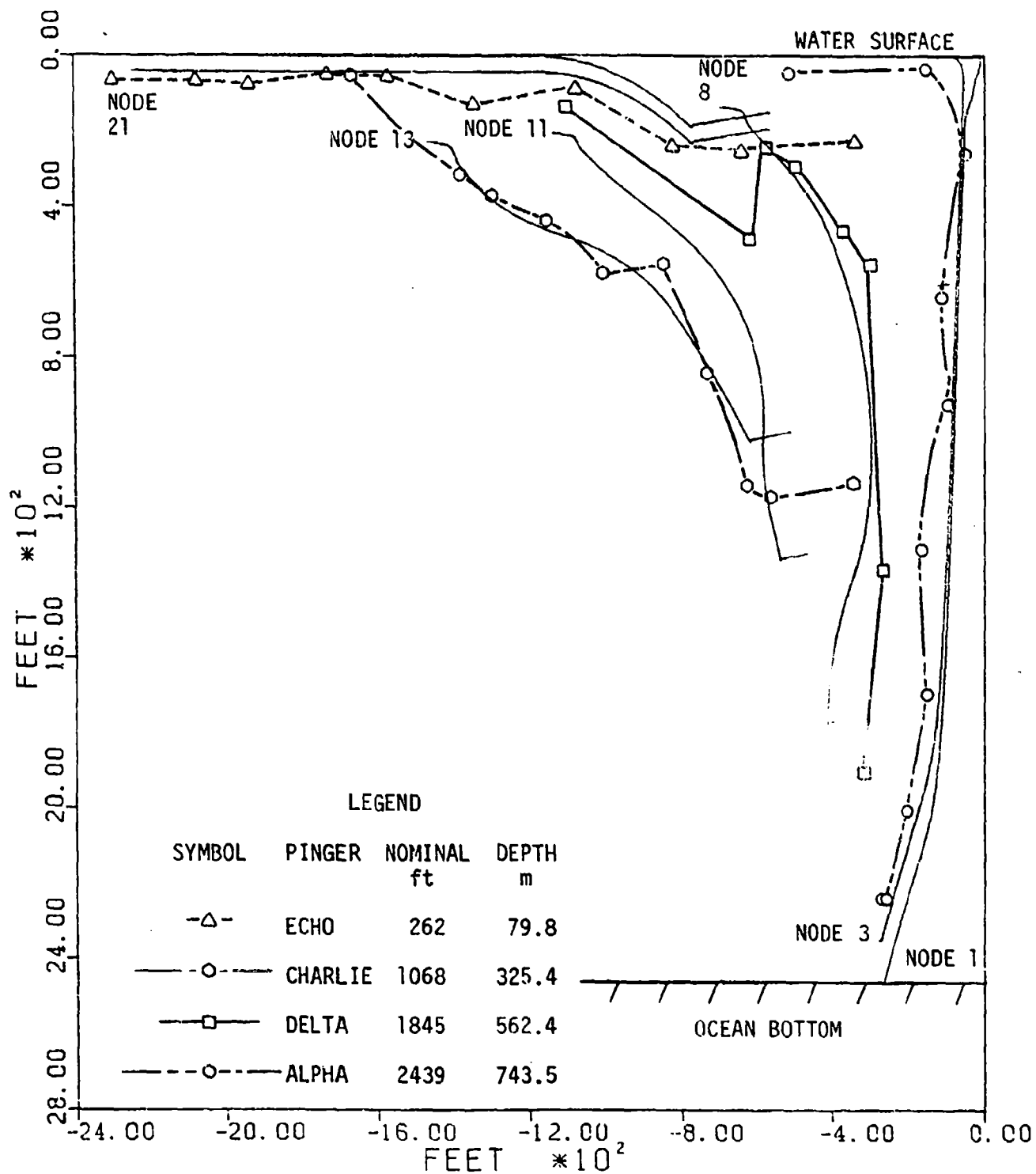


Figure 4-3. Trajectories of Major Nodes
(Composite)

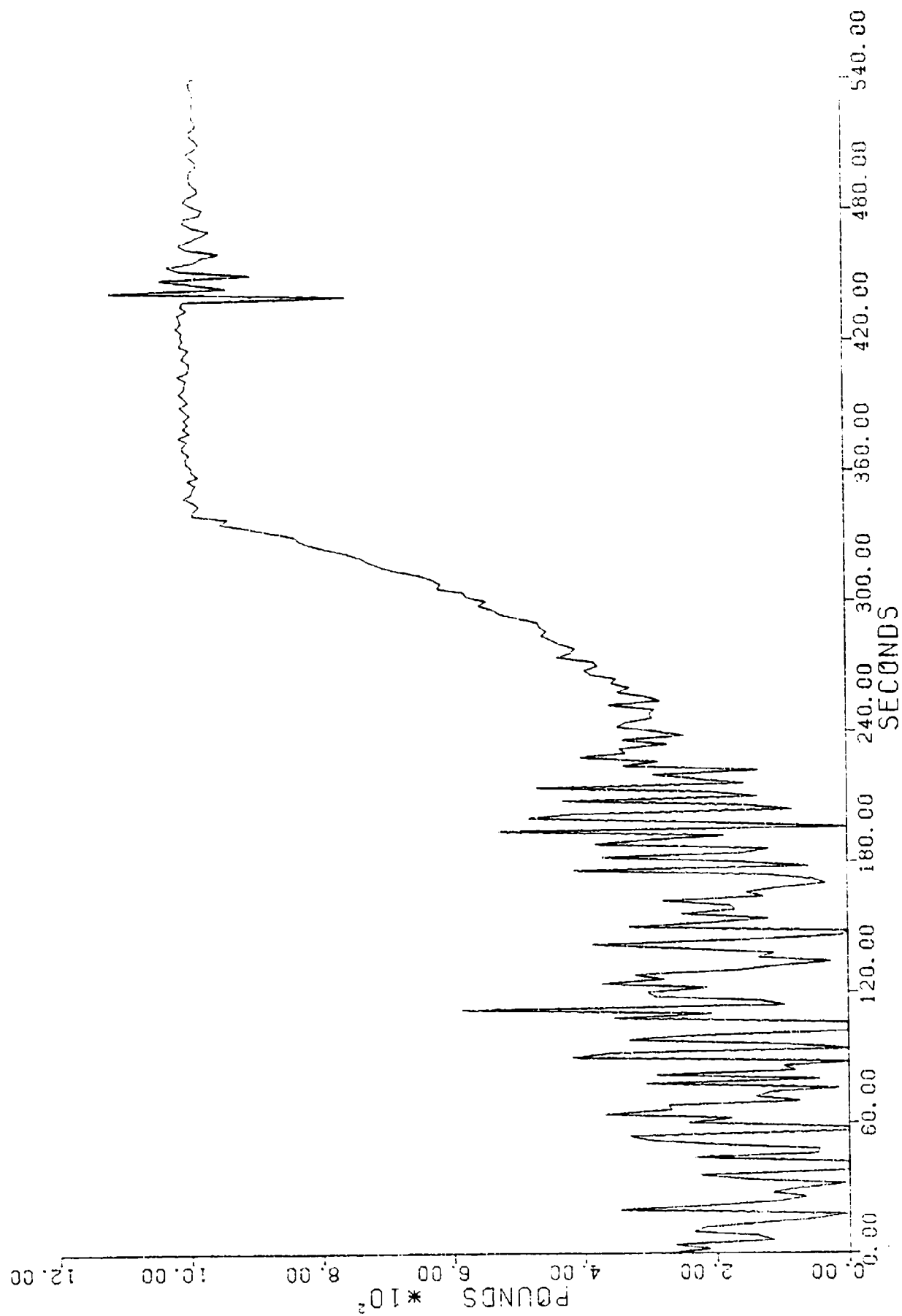


Figure 4-4. Calculated Tension in Element Twenty-One (FVR 1)

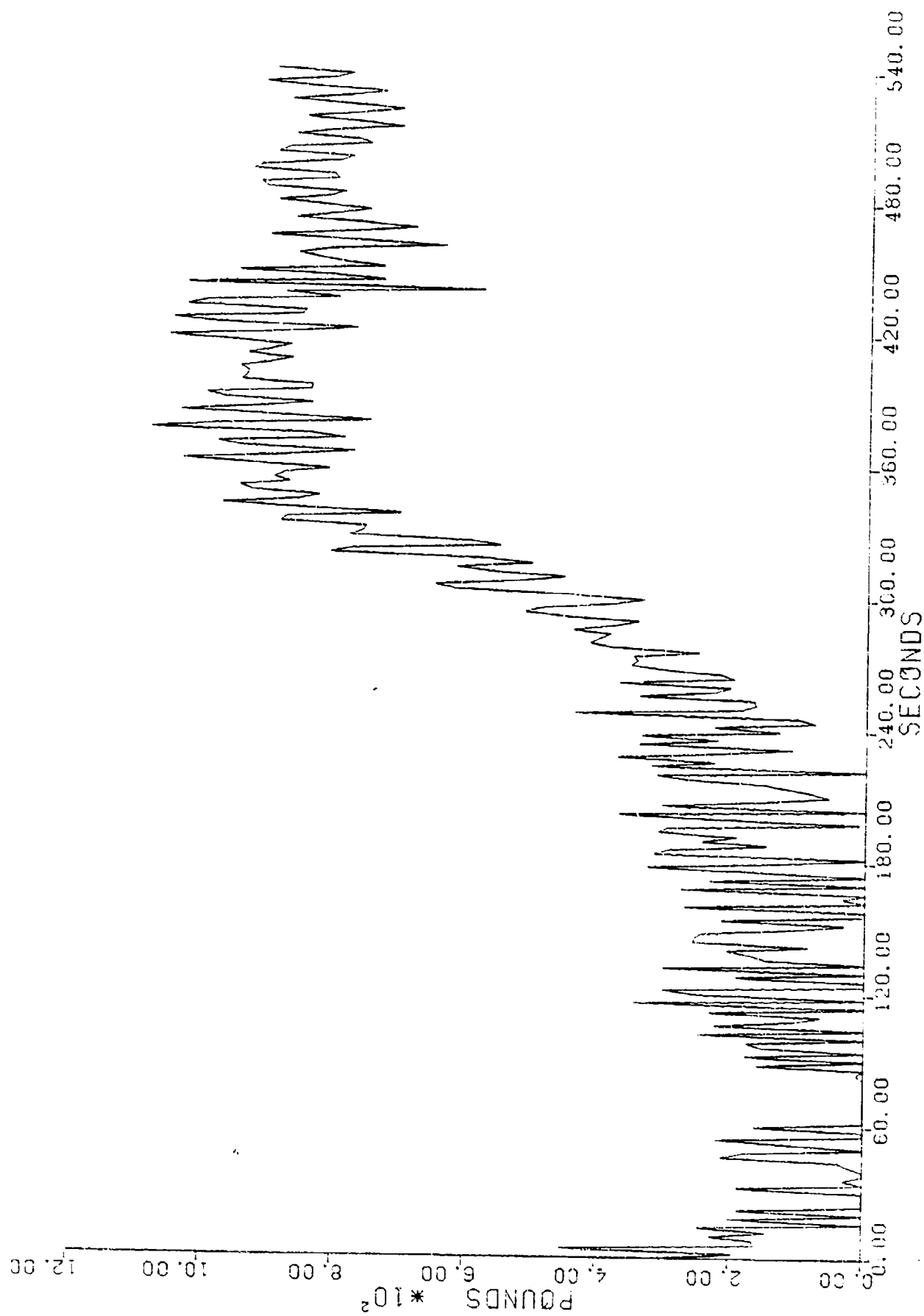


Figure 4-5. Calculated Tension in Element Thirteen (FVR 2)

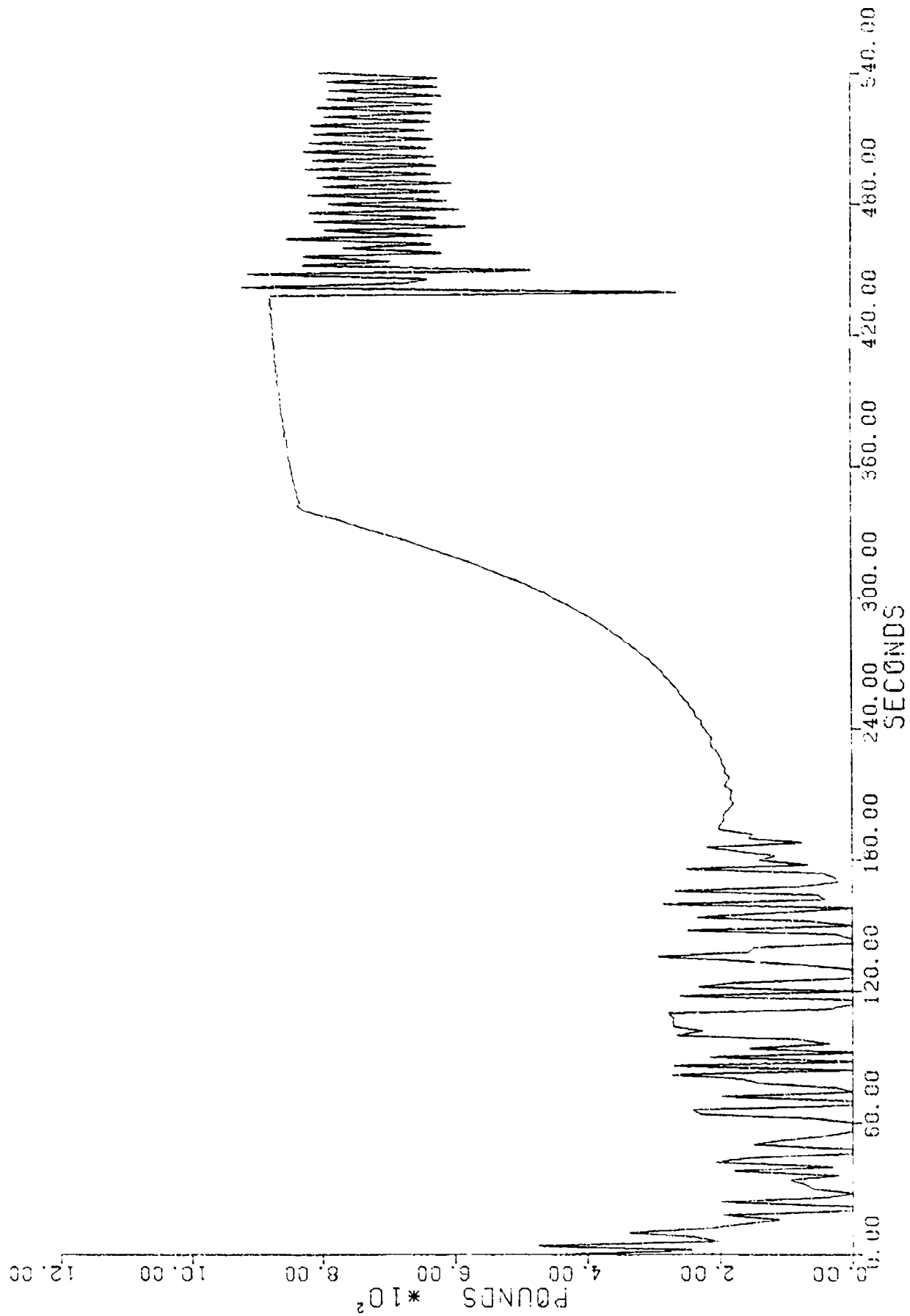


Figure 4-6. Calculated Tension in Element Eight (FVR 3)

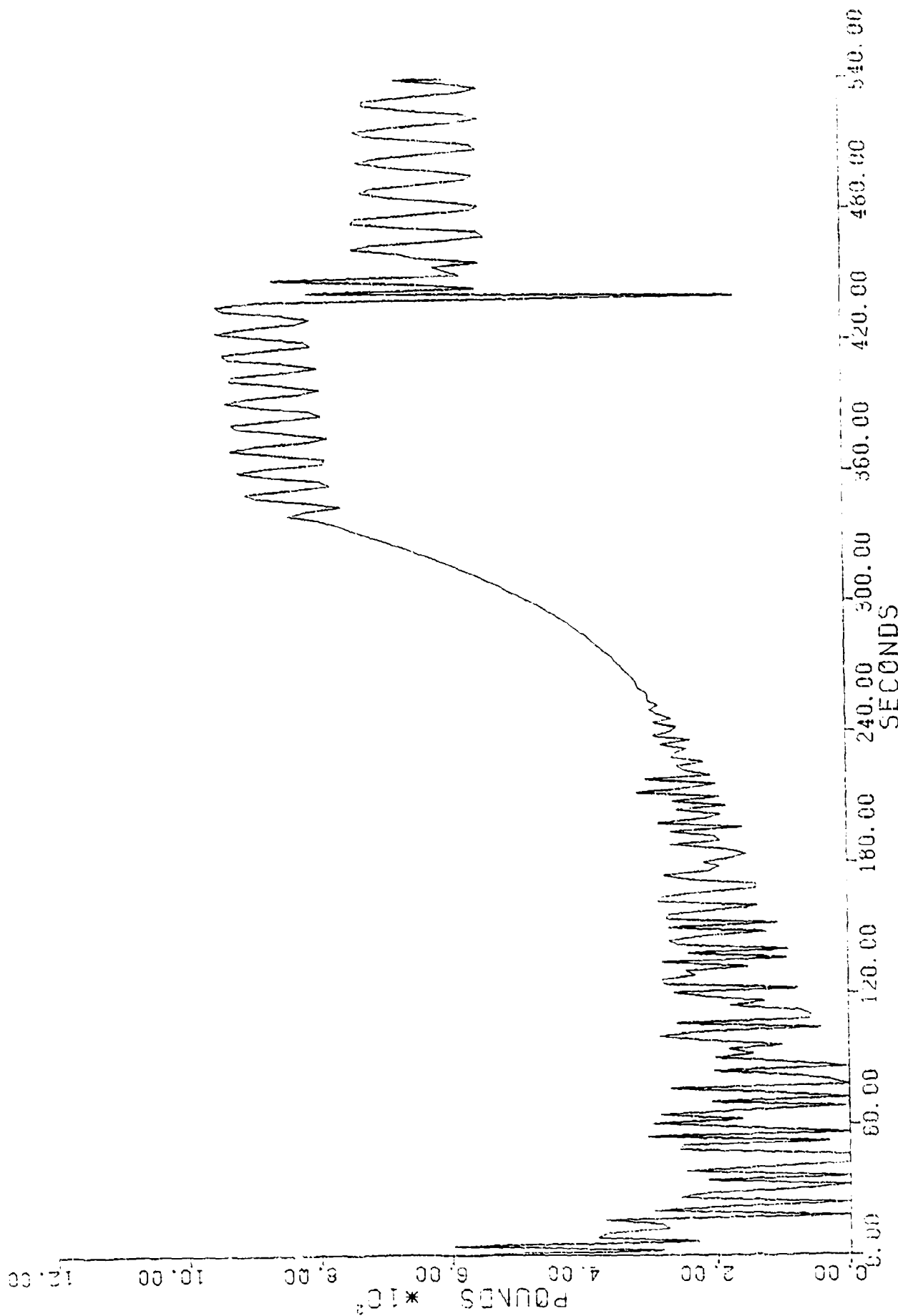


Figure 4-7. Calculated Tension in Element Three (FVR 4)

The large, undamped oscillations of tension shown on Figures 4-4 through 4-7 (especially Figure 4-5) are artifacts of the SEADYN model.

It is believed that these oscillations represent the resonant exchange of elastic energy between adjacent elements. This energy is dissipated in nature by material damping, i.e., hysteresis in the stress-strain curve of the element material. The SEADYN algorithm does not currently include material hysteresis.

The drag coefficient of the anchor and buoys was calculated (Appendix A) as part of the input model to produce terminal velocities equal to those measured in MDE, so the time from release to impact is, not surprisingly, equal on Figures 2-4 through 2-7 and Figures 4-4 through 4-7.

However, the beginning and duration of sub-events may be usefully compared, after aligning the impact pulse. For example, both data and model indicate that a very low tension occurs 16 to 18 seconds after anchor release. Figure 2-6 shows the main buoy pulled under 97 seconds before impact. This is marked by the change from large, wave - induced tension pulses to smaller double pulses after immersion (tension waves echoing off the massive main buoy). Buoy immersion is shown as 96 seconds before impact on Figure 4-5 from the SEADYN results.

The post-impact "ringing" has a four second period, as shown on the FVR plots in Section Two. The corresponding plots in Section Four show a period of about 4.5 seconds for the first few oscillations after impact. This "ringing" dies out after 3-4 cycles on the FVR plots and either dies out or is replaced by a spurious oscillation on the SEADYN plots within four cycles of impact.

At the start of the anchor drop the vertical force exerted by the falling anchor is turned by the "water sheave" principle into a roughly horizontal force on the main buoy. The tension is defined primarily by the hydrodynamic drag tangent to the cable and nodes. But as the anchor falls deeper and the water sheave is worn away, the cable trends more and more towards the vertical. The main buoy is pulled deeper in the water until it comes awash and submerges. Both model and data reflect this smooth increase in tension followed by a period of roughly constant tension until the anchor impacts on the bottom.

Figures 4-8 through 4-11 show the FVR data superimposed on the SEADYN element tensions.

4.4 Computer Aspects

This problem was duplicated on a very large vector-processor. Although the time to compile SEADYN was reduced from 20 seconds to five seconds, the execution time increased slightly. The cost to rewrite the SEADYN code in order to better use the vector-processor will barely offset the increased unit cost of that machine.

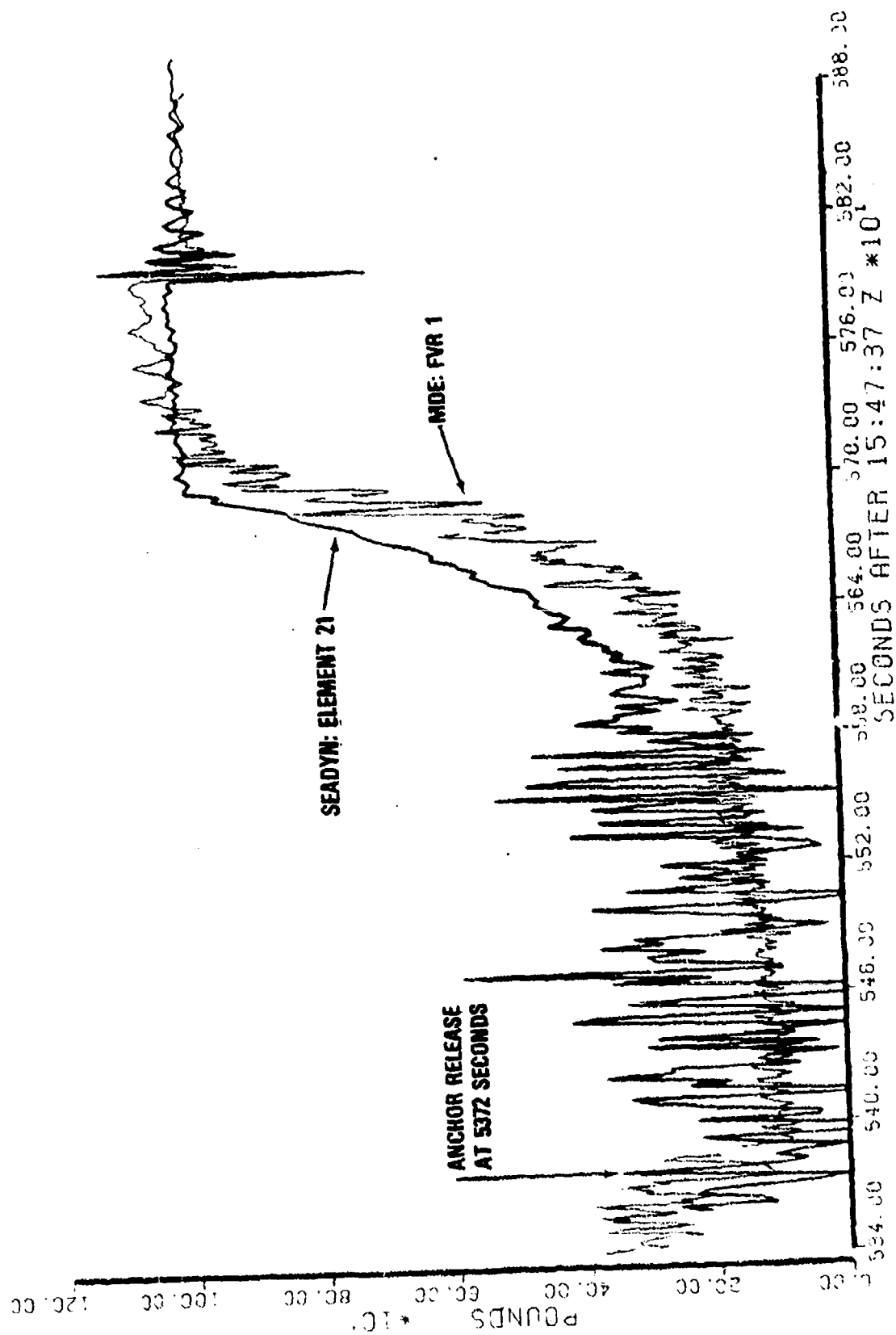


Figure 4-8. Tension Comparison for FVR 1

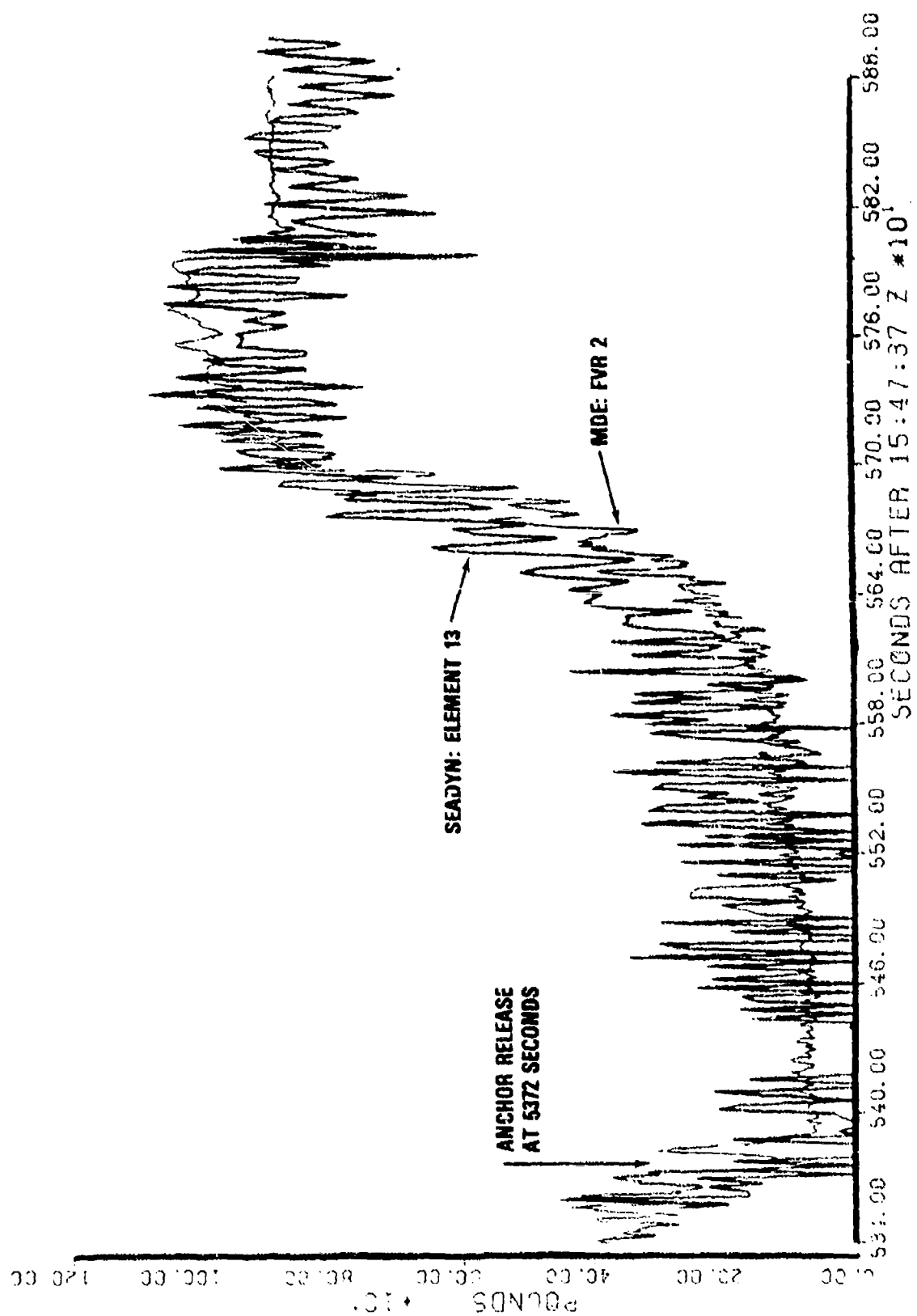


Figure 4-9. Tension Comparison for FVR 2

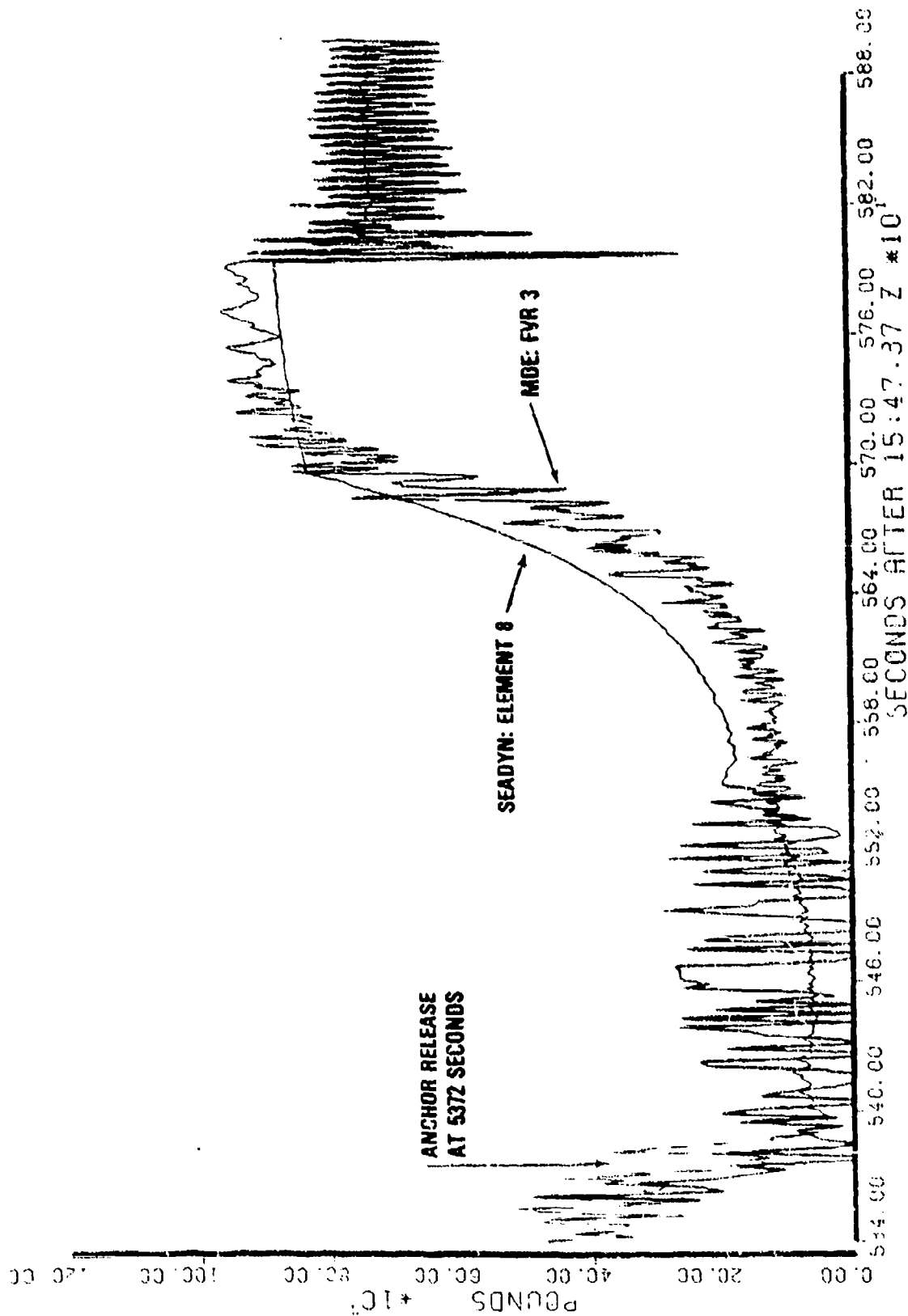


Figure 4-10. Tension Comparison for FVR 3

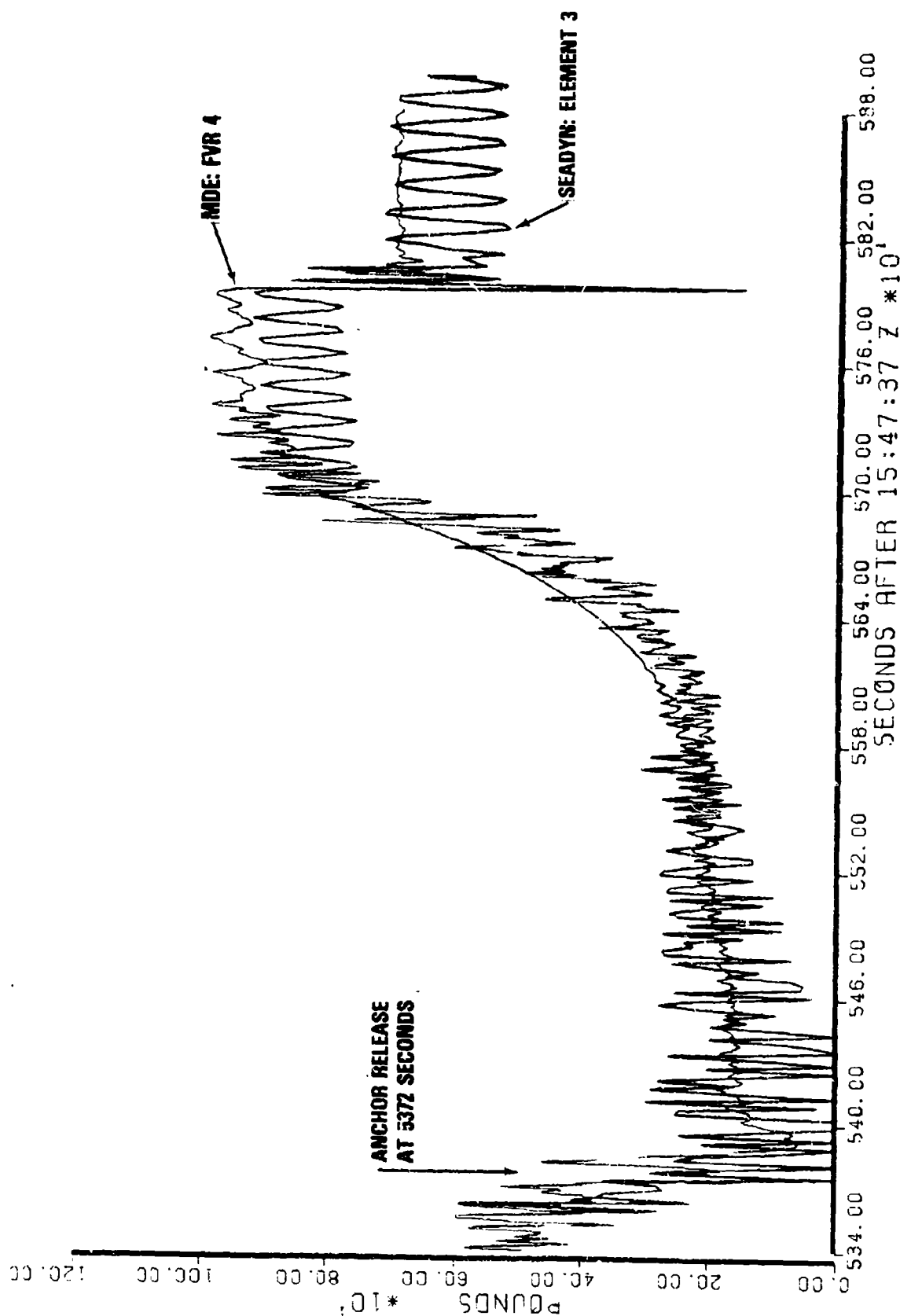


Figure 4-11. Tension Comparison for FVR 4

SECTION 5

CONCLUSION

The MDE test report cited in Section Three set the challenge that the MDE data formed "a convincing test" a mooring dynamics model, especially the FVR tension plots. The figures and comparisons drawn in Section Four show that in many respects SEADYN has met the challenge laid down by those words. However, some cautions are in order:

- Better damping of inter-nodal tension waves is a major need. Much information is being masked behind the spurious oscillations.
- The modeling of a physical system into equivalent SEADYN nodes is not trivial. Each problem must be approached with care. Technical skills are required in the field of hydrodynamics in order to successfully use SEADYN.
- The selection of SEADYN options for a successful "run" likewise is not trivial. At this time novice users require extensive coaching from more experienced users.

REFERENCES

1. Taylor, B.D., H.S. Zwibel, and D.J. Meggitt, "Research Plan for the Dynamic Response of Cables Suspended in the Ocean", Civil Engineering Laboratory, December, 1974.
2. Palo, P.A., "Comparisons Between Small-Scale Cable Dynamics Experimental Results and Simulations Using SEADYN and SNAPLG Computer Models", Civil Engineering Laboratory TM M-44-79-5, January, 1979.
3. Buck, E.F., and D.J. Meggitt, "Laboratory Experiments on the Large Displacement Dynamics of Cable Systems", Civil Engineering Laboratory TM M-44-78-6, February, 1978.
4. Meggitt, D.J., and D.B. Dillon, "At-Sea Measurements of the Dynamic Response of a Single-Point Mooring During an Anchor-Last Deployment", Civil Engineering Laboratory TM 44-78-9, March, 1978.
5. Webster, R.L., "Deep Sea Ship Moor Acceptance Report SEADYN/DSSM", Volumes 1-4, Ocean Engineering and Construction Project Office Report FP0-1-78(16), Chesapeake Division, Naval Facilities Engineering Command, August, 1978.
6. Walden, R.G., D.H. DeBok, D. Meggitt, J.B. Gregory and W.A. Vachon, "The Mooring Dynamics Experiment - A Major Study of the Dynamics of Buoys in the Deep Ocean," Paper No. 2883, Proceedings of Offshore Technology Conference, 1977.

APPENDIX A

MODELING MDE EXPERIMENT FIVE FOR SEADYN

A.1 Assigning The Nodes

Given an overall length of cable in a system, the user must select the number and location of nodes to be included in his input model. There will usually be a fairly obvious minimum number of nodes, located at cable ends and Y's and where discrete bodies are attached. But more nodes will usually be required in order to express the dynamic curvature of the cable adequately.

However, there is a double penalty extracted for using more nodes. On the one hand, more nodes mean more computation in each "pass" along the cable. On the other hand, more nodes mean shorter elements. There is a direct relationship between element length and time step size. Shorter elements require shorter time steps. The number of time steps required to model a given time interval therefore increases with the number of nodes used in the model. When the user defines more nodes, the computer executes more passes requiring more computation.

The user relies on experience, intuition, and the results of trial runs to concentrate nodes in areas of sharpest curvature.

Figure 2-1 shows the CEL mooring as it was deployed during the MDE. Figure 3-2 shows the mooring as it was modeled for SEADYN. By comparing these figures, it will be seen that nodes were located where one or more instruments were clustered. Long wire rope spans were broken into uniform elements between 100 and 200 feet long.

The center spans were assigned longer elements than the spans near the upper and lower ends, because the cable curvature is greatest near the ends in this problem. Element lengths less than 100 feet were accepted when they could not be avoided, namely, elements 1, 2, and 21 where the node spacing defies the element. Element lengths were made long enough that the transit time for a tension wave along an element is at least .01 seconds. This allows a .005 second time step to be used in SEADYN.

A.2 Nodal Drag Coefficient

The terminal velocity of the combination of nodes 1, 2, and 3 is shown on Figure F-3 of Reference Four (page F-3). During the first two minutes, the descent speed is 6.14 feet/second. Later in the descent, the drag and buoyancy of other nodes slow the descent perceptibly.

From Figure 3-2, the net weight of nodes 1, 2, and 3 is $2600 - 611 - 790 = 1199$ LB. Using a familiar hydrodynamic expression in the form

$$C_D \cdot A_T = F / Q,$$

where F is force and Q is dynamic pressure,

gives

$$C_D \cdot A_T = 32.0 \text{ Ft}^2.$$

The actual anchor was made of sandbags heaped on a wooden pallet and contained by a coarse net. This irregular shape was approximated by a sphere four feet in diameter. The diameter of the sphere was selected to coincide with the length of a side of the pallet. The spherical shape was assumed to approximate the shape of the sandbag pile. SEADYN is able to calculate the added mass coefficients for spheres. Combining the frontal area of the anchor, assumed to be a four foot diameter sphere, with the areas of the components in nodes two and three gives

$$A_T = 12.6 + 16.3 + 12.1 = 41 \text{ ft}^2,$$

so that

$$C_D = 32/41 = 0.78.$$

It is assumed that this coefficient applies to all the nodes, not only nodes 1, 2, and 3 as computed.

A.3 Nodal Weight

The weight of each node is simply the sum of the weights of the parts. The weights and dimensions of the MDE components were taken from Reference Four, Table two, page 16. Table A-1 shows how these weights were assigned to each node.

TABLE A-1. NODAL PARAMETERS

NODE	COMPONENT	WEIGHT (LB.)	FRONTAL AREA (FT ²)	EQUIVALENT DIAMETER (FT)
2	Release 1	70.	2.14	4.56
	Release 2	70.	2.14	
	Frame (estimated)	20.	2.00	
	DC Pinger	76.	2.20	
	28" sphere	-847.	7.88	
		<u>611.</u>	<u>16.36</u>	
3	38" Sphere	-847.	7.88	3.92
	DC Pinger	76.	2.20	
	FVR	-4.	1.97	
	Chain Excess*	-15.		
		<u>-790.</u>	<u>12.05</u>	
8, 13	SC Pinger	44.3	1.15	2.15
	FVR	-4.	1.97	
	Chain	10.2	.51	
	Wire Excess*	-.5		
		<u>50.</u>	<u>3.63</u>	
11	T/P	20.0		.96
	Wire Excess*	.1		
		<u>19.9</u>		
21	SC Pinger	44.3	1.15	2.21
	FVR	-4.0	1.97	
	T/P	20.0	0.72	
	Wire Excess*	-.5		
		<u>59.8</u>	<u>3.84</u>	
22	44" Sphere	-1050.		3.67
	Chain Deficit*	4.		
		<u>1046</u>		

* Corrects for excess/deficit in element lengths adjusted to reach center of spherical node.

An element in SEADYN extends from the center of one node to the center of the next. As shown on Figure 2-1, the instruments were inserted in the line. Thus, the element lengths tabulated in Figure 3-2 are slightly too long. The weights of the nodes are adjusted downward to account for the weight of this extra length.

A.4 Equivalent Diameters

Table A-1 also includes the frontal areas of each nodal component. The equivalent diameter for a spherical node is calculated to give the same frontal area. Note that this diameter must not be used to calculate the "equivalent displacement" volume. That is why the weights used in SEADYN are immersed values.